AFRL-AFOSR-UK-TR-2012-0051

Developing Test Apparatus and Measurements of AC Loss of High Temperature Superconductors

Dr. Milan Polak
Dr. Pavol Kovac
Dr. Timothy Haugan

Institute Electrical Engineering
Slovak Academy of Sciences
Dubravska 9
Bratislava, Slovakia 84104

EOARD Grant 10-3079

Report Date: November 2012

Final Report from 27 August 2010 to 26 August 2012

Air Force Research Laboratory
Air Force Office of Scientific Research
European Office of Aerospace Research and Development
Unit 4515 Box 14, APO AE 09421

REPORT DOCUMENTATION PAGE

Form Approved OMB No. 0704-0188

1. REPORT DATE *(DD-MM-YYYY)*	2. REPORT TYPE	3. DATES COVERED *(From – To)*
8 November 2012	Final Report	27 August 2010 – 26 August 2012

4. TITLE AND SUBTITLE

Developing Test Apparatus and Measurements of AC Loss of High Temperature Superconductors

5a. CONTRACT NUMBER

FA8655-10-1-3079

5b. GRANT NUMBER

Grant 10-3079

5c. PROGRAM ELEMENT NUMBER

61102F

6. AUTHOR(S)

Dr. Milan Polak
Dr. Pavol Kovac
Dr. Timothy Haugan

5d. PROJECT NUMBER

5d. TASK NUMBER

5e. WORK UNIT NUMBER

7. PERFORMING ORGANIZATION NAME(S) AND ADDRESS(ES)

Institute Electrical Engineering
Slovak Academy of Sciences
Dubravska 9
Bratislava, Slovakia 84104

8. PERFORMING ORGANIZATION REPORT NUMBER

N/A

9. SPONSORING/MONITORING AGENCY NAME(S) AND ADDRESS(ES)

EOARD
Unit 4515 BOX 14
APO AE 09421

10. SPONSOR/MONITOR'S ACRONYM(S)

AFRL/AFOSR/EOARD

11. SPONSOR/MONITOR'S REPORT NUMBER(S)

AFRL-AFOSR-UK-TR-2012-0051

12. DISTRIBUTION/AVAILABILITY STATEMENT

Distribution A: Approved for public release; distribution is unlimited.

13. SUPPLEMENTARY NOTES

14. ABSTRACT

To reduce the weight of electrical power conductors for use on airborne platforms, high-temperature superconductor coated wires using YBa2Cu307-x (YBCO) show promise. The main obstacle to their implementation is the AC loss at operating frequencies in the 230-400 Hz range characteristic of the airborne electrical power systems and generators. This project's objectives were threefold.
First, a calorimeter measuring system for AC loss was developed using custom construction of nonmagnetic/nonmetallic liquid nitrogen containers to measure evaporated nitrogen caused by power dissipation and tested using a special YBCO pancake coil; this was found to be sufficient for measurements after initial experiments determined some instability without external heating.
Second, AC losses in the coils made out of YBCO superconducting wires were studied, confirming the simulation method used to calculate and predict AC loss and hysteretic effects of pancake coils and providing information on the coupling and hysteretic currents in the superconductor.
Third, distribution of magnetization currents in samples of conductors was studied by producing, using laser ablation, multifilament superconducting samples with various filament widths, with and without superconducting bridges between filaments. The bridges increase the reliability of the wires by allowing the electric current to circumvent a defect in a given filament without rendering the whole length of the filament inoperative.
Different methods of post-ablation treatment, such as oxygen annealing were tested in order to determine their effect on AC loss reduction. Results showed that the AC loss in multifilament superconducting wires can be very effectively reduced in proportion of the number of filaments. The oxygen annealing eliminates the residual coupling losses by converting the electrically conducting metal in the grooves segregating the superconducting filaments into insulating metal oxides. The strategically placed superconducting bridges between the filaments do not increase significantly the AC loss relative to the samples without such bridges.

15. SUBJECT TERMS

EOARD, high temperature superconductors, superconducting coils, AC loss, YBCO, calorimetry

16. SECURITY CLASSIFICATION OF:			17. LIMITATION OF ABSTRACT	18, NUMBER OF PAGES	19a. NAME OF RESPONSIBLE PERSON
a. REPORT	b. ABSTRACT	c. THIS PAGE			Victor B. Putz, LtCol USAF
UNCLAS	UNCLAS	UNCLAS	SAR	64	19b. TELEPHONE NUMBER *(Include area code)* +44 (0)1895 6160013, DSN 314-235-6013

Institute of Electrical Engineering
Slovak Academy of Sciences
841 04 Bratislava, Dúbravská cesta 9, Slovak Republic

Performance report

Developing Test Apparatus and Measurements of AC Loss of High Temperature Superconductors

Award No. FA8655-10-1-3079, European Office of Aerospace Research and Development (EOARD)

Program manager: Scott Dudley

Principal investigator: M. Polák, P. Kováč – part of evaluated period

Research team: J. Šouc, J. Kováč, P. Mozola, D. Erbenová, J. Talapa

Collaboration: P. Barnes, AFRL/RQPM
T. Haugan, AFRL/RQPM
J. Murphy, AFRL/RQPM and University of Dayton Research Inc.
G. Levin, AFRL/RQPM and UES Inc.

Bratislava, September 2012

Table of contents

1. List of Tables
2. List of Figures
3. Methods and Procedures
4. Results and discussion
5. Conclusions

References

Memorial for Milan Polak (1937 - 2012)

Appendix

Publication: J. Murphy et al, IEEE Trans. Appl. Supercond., Oct. 2012

Publication: G. Levin, et al, IEEE Trans. Appl. Supercond., Oct 2012

Annual Report: 16 Aug 2011

Report: EOARD Window-on-Science Visit for P. Mazola, Oct 2010

1. List of Tables

Table 1: List of examined samples

2. List of Figures

Fig. 1 Simplified measurement scheme for dc characterization

Fig. 2 a/ edges after cutting……..b/ etched edge

Fig. 3 Schematic measurement set up and photo of ac loss apparatus

Fig. 4 a/ $I_c(B\perp)$ dependences of samples from set I
b/ $I_c(B\perp)$ dependences of samples from set II
c/ $I_c(B\perp)$ dependences of samples from set III
d/ $I_c(B\perp)$ dependences of samples from set IV

Fig. 5 Ac loss of samples from Set I (non-ideal part and good part) in Q and G representation before and after annealing

Fig. 6 ac magnetization loss of samples from set II

Fig. 7 ac magnetization loss of samples from set II -

Fig. 8 ac magnetization loss of samples from set III

Fig. 9 ac magnetization loss of samples from set IV in Q and G representation, and influence of etching is shown

3. Methods and Procedures

Laser Striated Coated Conductors

Four sets of $YBa_2Cu_3O_{7-x}$ (YBCO) coated conductor (CC) tapes were filamented by laser striation, and characterized by both dc and ac experimental methods. Description of the striated samples are listed in Table 1, and details of the striation process are given following.

The grooves in coated conductors were cut with a 355 nm wavelength pico-second laser, since it provided the cleanest and most narrow cuts available to us. Cutting was performed in an oxygen atmosphere because it was expected to oxidize material heated by the laser and prevent metallic copper or silver from collecting in the groove which could cause shorts between the filaments.

The laser cut itself on the tapes is about 12 μm wide and the cut affected zone is 13 μm to 13.5 μm wide. Typical filament width averaged about 73 μm and 45 μm. The cuts were made in two 39.5 mm sections resulting in an overall striation length of about 78 mm due to some overlap of the two sections. Depth of cuts were measured with a Veeco white light interferometer and was typically 24 μm deep except for occasional bits of debris which should have been oxidized by the oxygen rich atmosphere. The O_2 concentration was enhanced by blowing a very substantial stream of O_2 across the laser impact point.

For 'bridged' samples listed in Table I, the cuts were interrupted in a staggered pattern to permit limited current cross flow between filaments.

Table 1. Description and details of the examined samples.

Set of samples	Samples in set	Stabilize Layer	Filament Width [μm]	Note
Set I	Good part Non ideal part	Ag Ag	500 500	ac measurement before and after annealing in O_2
Set II	MM2012008 MM2012009 MM20120010 MM20120011	Cu Cu Cu Cu	200 150 100 70	Ac measurement of MM2012008 before and after sample ends etching
Set III	Set III/1 Set III/2	Cu Cu	73 43	
Set IV	Set IV/1 Set IV/2	Cu Cu	70 bridged 40 bridged	Ac measurement of Set IV/1 before and after sample end etching

DC characterization

Before AC loss measurements were done, direct current (dc) measurements were first performed for each sample of critical current (I_c) as a function of external dc magnetic field (B_{dc}). This was necessary because current leads were soldered to the non-striated parts (ends) of the samples, which were cut before ac measurement to exclude non-striated parts influence on ac loss results.

Standard 4-probe methods were utilized for I_c measurements. Magnetic field B_{dc} was oriented perpendicular to the wide surface of the sample and was changed from 0 mT up to 144 mT. Critical current I_c was measured for both direction of the dc current flowing in the sample (except samples from Set I), to check the "anisotropy" of pinning centers. The results show only a weak dependence of the critical current on the direction of the current flow. Samples were cooled down in liquid nitrogen. The distance between voltage taps was around 9 cm. The criteria for I_c estimation was 1μV/cm. A simplified measurement scheme is shown on Figure 1.

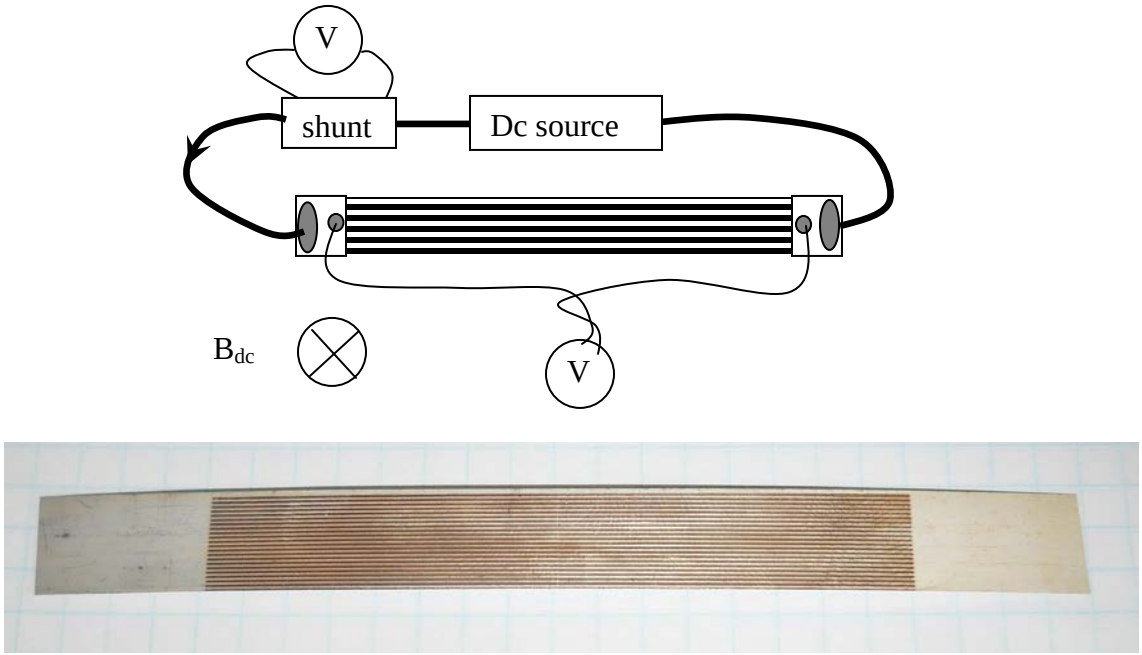

Figure 1. **(top)** Simplified measurement scheme for dc characterization.
(bottom) Example of YBCO striated sample with 12 mm width.

AC characterization

Ac characterization consists of alternating current (ac) magnetization loss P measurement and dependence on ac external magnetic field B_{rms} at two different frequencies f = 72 Hz and 144 Hz (36Hz and 72 Hz for samples from Set I). Ac field was varied from 0 mT up to 70 mT root-mean-square (rms). To see only influence of the striation on ac loss of the samples, the non-striated ends were cut before ac loss

measurement. Although according to optical photos the edges after cutting were "clear" (without electrical connection between superconducting paths), as shown in Figure 2a for some examples. In other samples edges were also etched completely to the substrate to remove the potential Cu or other remains, as shown in Figure 2b. Ac loss measurement of these two samples was performed before and also after this etching.

Original calibration free apparatus introduced for the first time in our lab was utilized for ac magnetization loss measurements. This method is based on the measurement of a part of the power supplied by the AC source to the AC magnet generating the magnetic field in which the sample is placed. The measurement system consists of two identical ac copper magnets connected in series and two measurement pick-up coils wound in parallel with magnets windings. During measurement the complete system is immersed in liquid nitrogen. The principal schematic measurement set up and photo of the base part of the apparatus are shown in Figure 3. A sample is located in one of the magnet, the other one and pick-up coil serve as compensation. More details about the calibration free method for AC loss measurement are described in [1]. Ac magnetization loss was measured by a standard lock-in technique. The dimension of space for sample (hole of Cu magnet) is 3 cm × 10 cm allowing to measure ac magnetization loss of whole striated part of samples (1.2 cm × 8 cm). Loss of the sample is calculated as $P = U_{loss}*I_{mag}$ (U_{loss} – component of signal voltage from pick-up coils in phase with I_{mag}, I_{mag} – ac current of Cu magnets). Measured results were recalculated to the length 1 m. In presented graphs of ac loss dependences both representation $Q=P/f$ and more sensitive representation $\Gamma = Q/B_{rms}^2$ is used (B_{rms} is rms value of applied ac field and $Q = P/f$ is loss normalize by frequency).

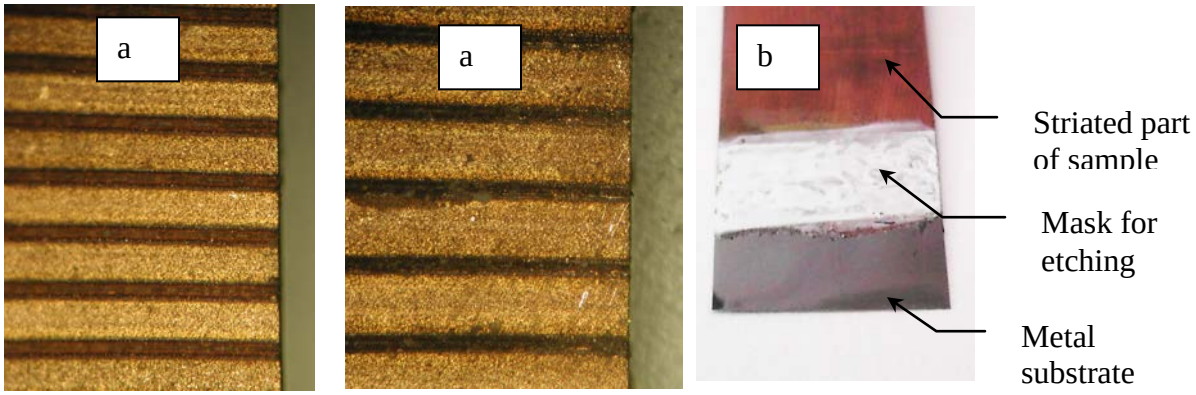

Figure 2. a/ examples of edges after cutting, and **b/** etched edge.

4. Results

4-1 Dc characterization

In Figures 2a – 2d $I_c(B_{dc\perp})$ dependences of all samples from individual Sets are shown. Logical I_c dependence on spacing is visible for all samples from SetII-SetIV related probably with the amount of removed supercoducting material. Bridging of the samples from SetIV has no influence on I_c. Good sample from SetI has evidently

stronger $I_c(B_{dc\perp})$ dependence. It can be explained that it is different sample then others and can have different kind of pinning centers.

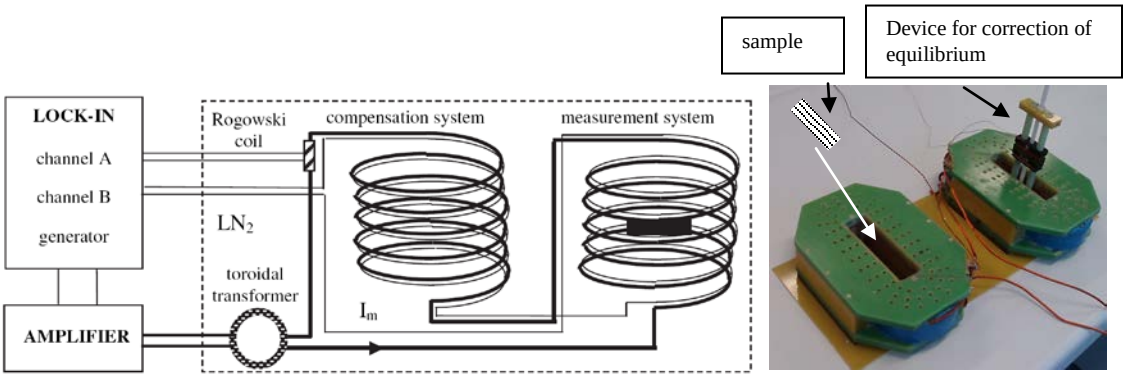

Figure 3. Schematic measurement set up and photo of ac loss apparatus.

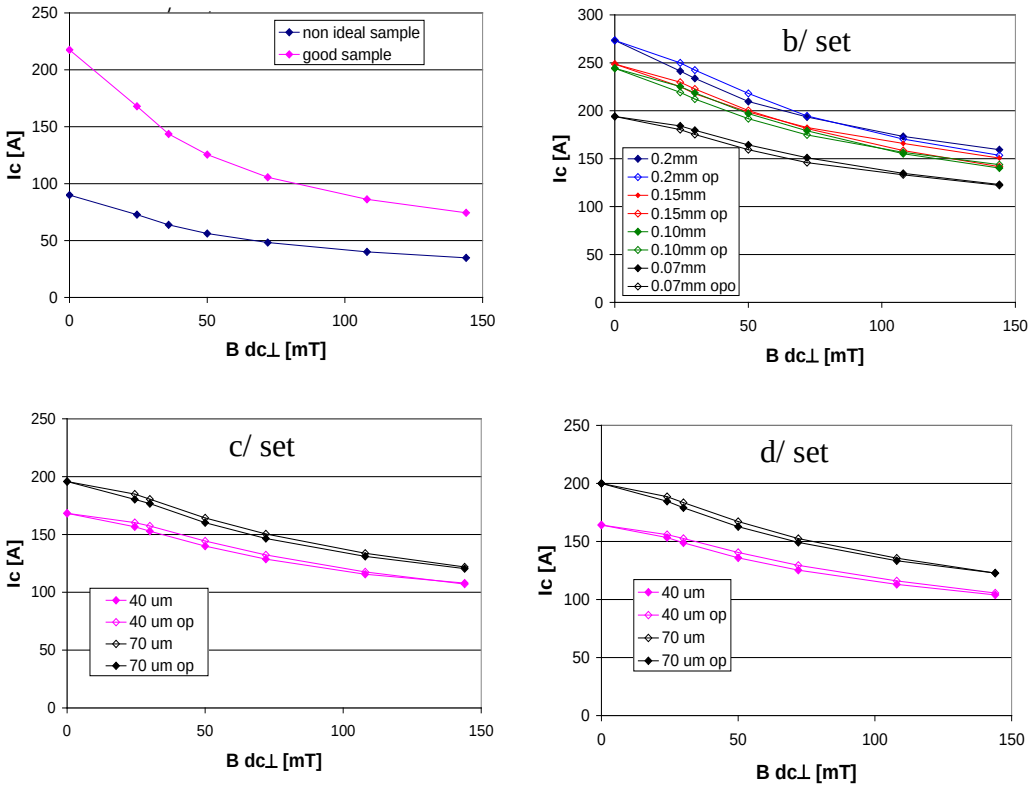

Figure 4. **a/** $I_c(B\perp)$ dependences of samples from set I
b/ $I_c(B\perp)$ dependences of samples from set II
c/ $I_c(B\perp)$ dependences of samples from set III
d/ $I_c(B\perp)$ dependences of samples from set IV

4-1 Ac characterization

SET I

Ac magnetization loss of both samples from Set I before annealing was similar. Frequency dependence is visible and can be ascribed to the coupling loss due to the conductive remains between superconducting paths, and due to the hysteretic character of superconductor loss $Q=P/f$ it should be frequency independent. A different situation was found after annealing. Whereas for non-ideal part samples ac loss after annealing only slightly decreased and frequency dependence remained, for good samples the frequency dependence disappeared and loss decreased radically. More, for good annealed samples the slope dependence of Q is about 3 confirming pure hysteretic loss of superconductor. Annealing procedure for this case is helpful in regard to ac magnetization loss.

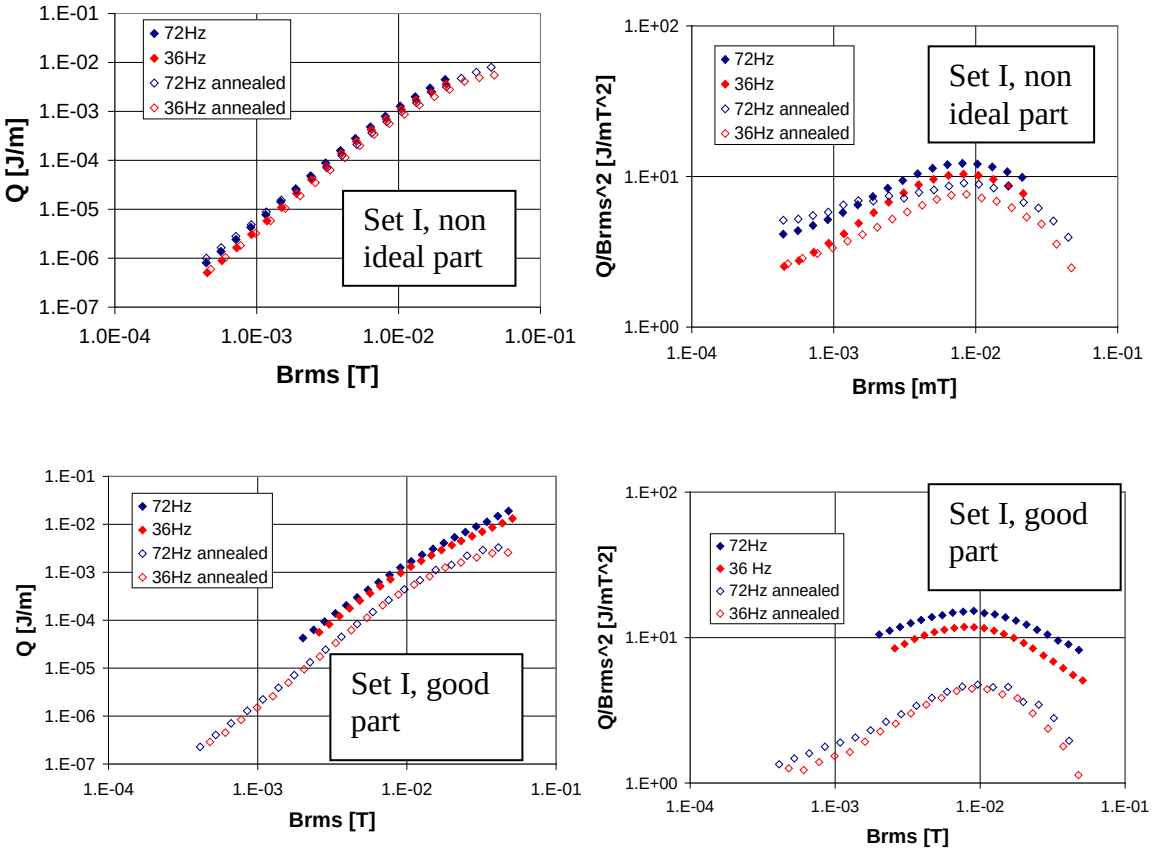

Figure 5. Ac loss of samples from Set I (non-ideal part and good part) in Q and Γ representation before and after annealing.

SET II

As is shown in Figure 6 for all samples of Set II strong frequency dependence was found confirming the presence of coupling currents. To avoid the influence of not proper cutting, the Cu layer from the ends of the sample with spacing 0.20 mm was etched;

however, this procedure had no effect as shown in Figure 7. To artificially connect the superconducting paths at the ends of this sample, in the next step they were soldered on the whole width. Increase of the loss was measured in this case and definitely confirmed that cutting was proper and had no influence on ac magnetization loss.

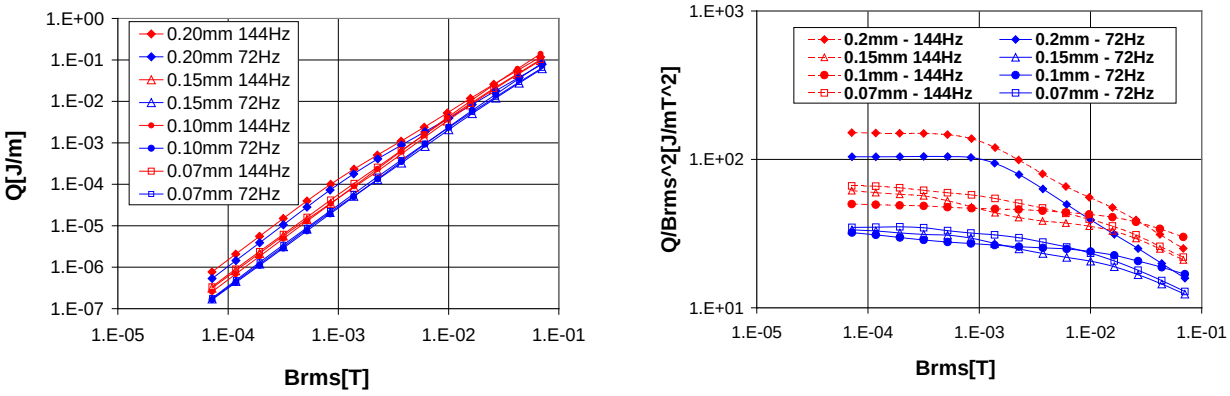

Figure 6. Ac magnetization loss of samples from set II in Q and Γ representation

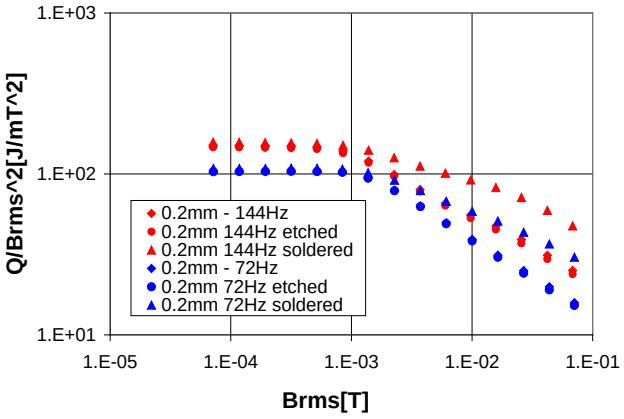

Figure 7. Ac magnetization loss of samples from set II – influence of ends etching and soldering

SET III

In Figure 8 ac magnetization losses for samples of Set III are shown. Also, they are compared with ac loss of a non-striated sample. As one can anticipate, no frequency dependence was found for the non-striated sample from the slope of Q dependence B_{rms} between 3-4, and not even in graph with more sensitive representation. On the contrary,

this slope for both striated samples is 2 and the losses are proportional to the frequency of applied ac magnetic field (two times higher *f*, two times higher loss). In the whole examined range of the magnetic field *B* one sees that the striated samples have much lower loss than the non-striated sample. Because for examined samples it is true only for higher field and because character of ac loss dependence is not typical for hysteretic loss, one can conclude that coupling loss dominates in the whole range (and loss of superconductor is not visible). Taking into account "clear" cutting, the measured loss of striated samples can be regarded as coupling losses due to conductive remnants between superconducting paths as a result of laser pattering. Anyway, striated samples have around one order lower loss comparing to non-striated one at higher examined ac field.

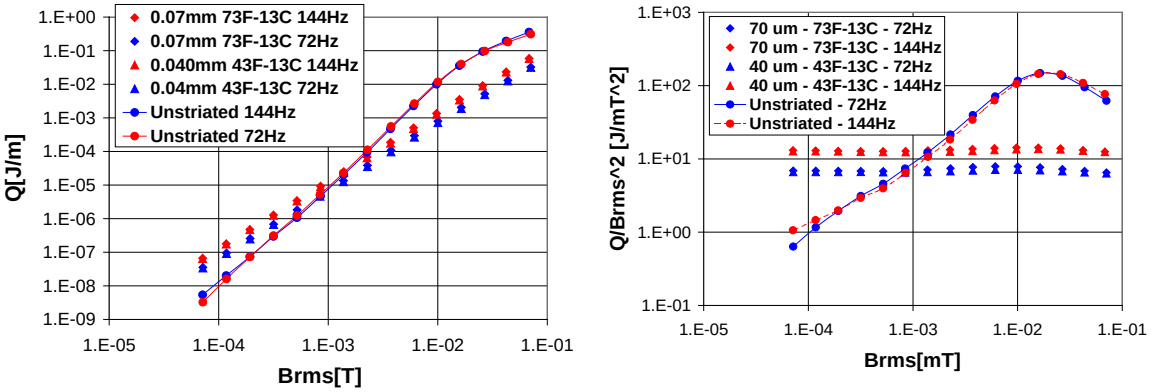

Figure 8. Ac magnetization loss of samples from set III in Q and Γ representation.

SET IV

Bridged samples from Set IV have similar ac loss behavior like samples from Set III (frequency dependence, dependence character). Precision of the non-striated part cutting before ac magnetization loss measurement was confirmed also on one sample from this Set (sample 70 μm spacing) – Figure 9. No change of ac loss dependence was found after ends etching completely to the metal substrate (dependences represented by diamonds signs and full lines with circles are practically the same).

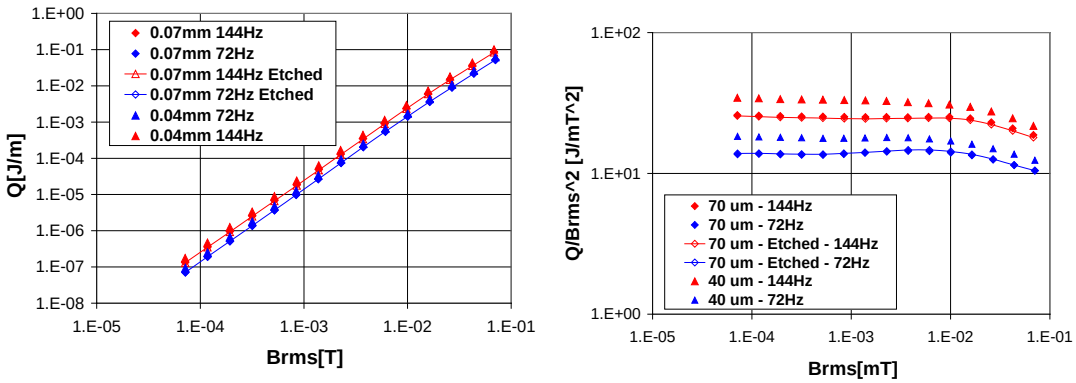

Figure 9. Ac magnetization loss of samples from set IV in Q and Γ representation, influence of etching shown as well.

5. Conclusions

Logical I_c dependence on spacing is visible for all samples from Set II - Set IV related probably with the amount of removed superconducting material. Bridging of the samples from Set IV has no influence on I_c. The good sample from Set I has evidently stronger $I_c(B_{dc\perp})$ dependence. It can be explained that it is a different sample than the others and can have different kind of pinning centers.

Striation for lowering ac magnetization loss is very effective for annealed samples from Set I (stabilized with Ag). For the good sample not only loss is decreased but also frequency dependence disappeared indicating no coupling loss (no conducting contacts between superconducting paths). Decreasing of ac loss was observed also for other samples from Sets II-IV (stabilized by Cu), but for all of them frequency dependence is visible. Character of loss indicates that mainly coupling loss contributes to these dependences. After successful elimination of the remnant conductive connections between superconducting paths created from laser patterning, additional ac loss reduction could be achieved.

In summary, a non-feedback (brute) force approach was attempted to making copper stabilized multifilament coated conductors with the stripe width varying from 200 μm to 40 μm using laser ablation to cut grooves through 20 μm thick Cu stabilizer. The critical current in striated samples decreases with magnetic field not as rapidly as in non-striated samples, indicating increased pinning strength caused by edge barrier effect or by increased number of defects appearing as the result of laser ablation.

The total loss decreases with increasing number of stripes, but the loss per unit of the critical current is about the same as in striated samples with 1 mm wide stripes. Even if cost is not an issue, striation by laser ablation beyond this limit seemed to be ineffective in this first attempt, and this method has to be refined or other methods of manufacturing more finely striated coated conductors are needed. Results of these studied and developing cryogenic pieces for an AC loss spin-around-magnet (SAM) machine were presented at the Applied Superconductivity Conference (ASC) 2012, and also submitted for publication to IEEE Transactions on Applied Superconductivity [Ref. 2,3].

References

Note - complete papers listed below are included in the Appendix and appended.

1. J. Šouc, F. Gömöry, and M. Vojenčiak, "Calibration free method for measurement of the AC magnetization loss," *Supercond. Sci. Technol.* **18**, 592-595 (2005).

2. G.A. Levin, J. Murphy, T. Haugan, J. Šouc, J. Kováč, P. Kováč, "AC Losses of Copper Stabilized Multifilament Y-Ba-Cu-O Coated Conductors," *ASC 2012 Conference, Portland, Oregon, USA, October 7-12, IEEE Trans. Appl. Supercond.*, submitted, Oct 2012.

3. J.P. Murphy, M.J. Mullins, P.N. Barnes, T.J. Haugan, G.A. Levin, M. Majoros, M.D. Sumption, E.W. Collings, M. Polák, and P. Mazola, "Experimental Setup for Calorimetric Measurements of Losses in HTS Coils due to AC Current and External Magnetic Fields", *ASC 2012 Conference, Portland, Oregon, USA, October 7-12, IEEE Trans. Appl. Supercond.*, submitted, Oct 2012.

Memorial for Milan Polák

February 2, 2012. Slovak scientist, Dr. Milan Polák, passed away on January 31st, 2012, after a severe short illness. His rather sudden departure at 74 came as a sad surprise to his colleagues and co-workers in Slovakia and abroad. He has been well-known to the superconductivity community through his active studies of electromagnetic properties of superconductors, superconducting magnets and devices, in particular on AC losses and related problems.

Milan Polák was born in 1937 in Strekov, finished university studies in 1960, and got his Ph.D. in 1967 and the habilitation (D.Sc.) in 1989, both at Slovak Academy of Science (SAS) in Bratislava. From 1967 to 1969 he was in Giessen and Karlsruhe as Alexander von Humboldt Scholar, 1983 – 84 as lecturer at the L´Université National de Gabés in Tunis and 1992–95 as visiting scientist in the Applied Superconductivity Center, Madison. Since 1960 he is with the Institute of Electrical Engineering (IEE), Slovak Academy of Sciences in Bratislava, Slovakia.

Milan Polák (ca. 2011)

- Polák made significant contributions to applied superconductivity, *e.g.*, designed and tested NbTi coils for the generation of magnetic fields at industrial frequencies, AC loss measurements of superconductors and superconducting coils, development of low AC loss YBCO superconductors. He successfully managed several national and international research projects and published about 190 publications in international journals.

For 50 years he was active in the Institute Electrical Engineering of SAS and, to the end of his activity, liked the “hands on” experimental work in laboratory, which was a stimulating example also for much younger colleagues. He was also as a member of several scientific boards and, as the director of IEE, was also involved in effective reorganization of the Institute of Electrical Engineering at the time of “political change”.

Milan was a very creative colleague, and up to the end of his live stimulated others to useful activities. His colleagues and collaborators appreciated his experience and knowledge as well as his friendship and sense for humour. For this editor it was a special privilege to spend with him the time of his last MT-22 conference (Sept. 2011) and also in common experiments during his last years.

P. Kováč, Oct 2012

Appendix

INSTITUTE OF PHYSICS PUBLISHING SUPERCONDUCTOR SCIENCE AND TECHNOLOGY

Supercond. Sci. Technol. **18** (2005) 592–595 doi:10.1088/0953-2048/18/5/003

Calibration free method for measurement of the AC magnetization loss

Ján Šouc[1], Fedor Gömöry[1] and Michal Vojenčiak[2]

[1] Institute of Electrical Engineering, Slovak Academy of Sciences, Dúbravská cesta 9, 842 39 Bratislava, Slovak Republic

[2] Department of Power Electrical Systems, University of Žilina, Vel'ký diel, 010 26 Žilina, Slovak Republic

Received 30 November 2004, in final form 11 February 2005
Published 15 March 2005
Online at stacks.iop.org/SUST/18/592

Abstract

A *calibration free* measurement method for determination of the magnetization loss of superconducting samples exposed to the external AC magnetic field is presented. The idea is based on the measurement of the part of the power which is supplied by the AC source to the AC magnet generating the magnetic field, in which the sample is located. It uses a coil wound in parallel to the AC field magnet as the measurement coil. To achieve the necessary sensitivity, two identical systems are used, each consisting of an AC magnet and a measurement coil, one of them containing the sample and the other left empty. No measurement and/or calculation of the calibration constant is required. To confirm the suitability of this method, the loss of a Cu sample with known dissipation was measured. The applicability to the AC magnetization loss measurements of superconducting tapes is presented.

1. Introduction

Dissipation appears in different kinds of materials when these are exposed to AC magnetic field. This phenomenon, called AC loss, is of particular importance for superconducting wires considered for electrical power applications. It has direct consequences for the rated cooling power of cryogenic machines and thus the installation cost.

In the case when a superconducting wire transports an AC current, it is a source of electromagnetic field. Experimental determination of AC losses in this case is straightforward, based on the power balance in the wire as the only source of energy. From the voltage measured with the help of a pair of voltage taps, the component in phase with current is extracted. Multiplying this so called loss voltage by the current gives the loss power directly.

When the magnetization loss in a superconducting wire is to be determined experimentally, the sample is placed in a coil generating the AC field. This coil represents the source of energy. However, it is generally preferred to confine the measurement of power flow on the sample itself, working thus on the power balance in the load. The most exploited method for magnetization AC loss measurement at grid frequencies, offering excellent reproducibility and versatility, uses pick-up coils placed in the sample vicinity. Unfortunately, into the formula for AC loss determination from the pick-up coil voltage, a conversion constant reflecting the geometry and distribution of magnetization currents in the sample must be introduced. This conversion constant is obtained in different ways.

In [1] the standard soft magnetic sphere sample with known susceptibility and in [2] a paramagnetic compound were used. A uniformly magnetized sphere and the calculated total flux in the pick-up coil was utilized in [3]. Measurement of the eddy current loss of a normal conductor tape was performed in [4, 5]. A normal conductor wire loop fed with known alternating current was suggested for estimation of the calibration constant in [6–8]. In [9] the calibration constant was calculated for the case of a small sample for which the magnetization was approximated by a dipole. In the case of saddle-like pick-up coils the correct relation for loss was found [10–12]. In [13] a general solution for various kinds of pick-up coils was described in detail. In European Standards [14] calibration is performed with magnetization of a standard specimen.

Here we show that in an AC magnetization experiment it is also possible to determine the AC loss in the sample starting from the power delivered by the AC field source. In particular, we have found a rather simple way to detect the total AC loss in the system except the resistive loss in the AC field coil. The eddy current losses in the coil winding could be eliminated using the concept of a bridge, i.e. connecting in parallel two

0953-2048/05/050592+04$30.00

systems, one with the sample and one empty. Then, the true AC loss in the sample is obtained without the need of calibration factors, demagnetization factors or other scaling factors.

2. Experimental details

2.1. Basic idea

The losses in a sample exposed to an external AC magnetic field are covered by the power supply energizing the AC magnet [15, 16]. This was analysed in detail in [17]. In other words, the AC loss of the sample forms a portion of the AC power supplied to the AC field magnet. With a suitable procedure enabling us to distinguish it from the AC loss in the AC field magnet winding, the absolute value of the AC loss in the sample could be determined.

The main problem of such a calibration free measurement of the sample loss as the part of the supplied power is that it is generally much lower than the losses in the AC field magnet generating AC magnetic field. Our idea to overcome this obstacle is schematically shown in figure 1. In the straightforward method of AC power evaluation (figure 1(a)), the measured voltage is

$$V = RI_{\mathrm{m}} - \mathrm{d}\psi/\mathrm{d}t \qquad (1)$$

with the resistive component RI_{m} (R represents resistance of the AC field magnet) prevailing over the voltage generated by the change of magnetic flux ψ, linked to the AC magnet coil. To eliminate the first term on the right-hand side of formula (1), that is useless for the sample loss determination, we suggest to use the arrangement shown in figure 1(b), where

$$V = -\mathrm{d}\psi/\mathrm{d}t.$$

In other words, instead of taking the whole voltage from the magnet power supply we use the signal registered by a measurement coil wound in parallel with the AC field magnet. However, this measurement coil has no electrical contact with the AC field magnet coil. Then, it does not feel the resistive loss in the AC field magnet winding that generally represents the largest dissipation, which the power supply has to cover. The measurement coil exactly registers the inductive voltage on the winding, i.e. that given by the time derivative of the linked magnetic flux, ψ. Therefore, besides a strong inductive part due to the inductance of the magnet coil, it contains also the signals induced by the eddy currents in the AC field magnet winding and by the currents in the sample. Only the last term is of interest for us, therefore it is necessary to eliminate the remaining components. In our case, the other magnetic system—the compensation system—consisting of the compensation AC magnet and the compensation coil with exactly the same geometry as the AC field magnet and the measurement coil, representing the measurement system, is utilized. The compensation magnet is connected in series with the AC field magnet. The signal from the compensation coil is subtracted from the signal measured by the measurement coil—figure 2, leaving the sample loss as the only remaining component of the signal measured after such compensation. A significant feature of this arrangement is that the measured signal will represent directly the power supplied by the source to cover the sample AC loss (in other words the measured signal should be zero in the reference case when the sample is not inserted into the AC field magnet). Therefore, the suggested method is a direct measure of the true AC loss.

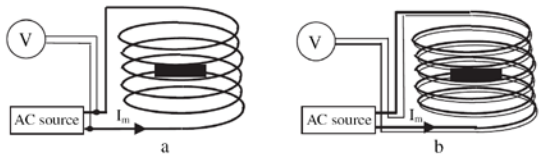

Figure 1. Set-up magnetization loss determination in the superconducting sample (black rectangle) based on the measurement of power supplied to the AC field magnet. (a) Measurement of total AC power delivered by the AC power supply; (b) modification to neglect the resistive loss in the AC field magnet.

2.2. Experimental apparatus

The measurement set-up is shown in figure 2. It is designed to determine the magnetization loss at 77 K, thus the whole coil system is immersed in liquid nitrogen. The DSP lock-in amplifier 7265 (EG&G Instruments) was used as a basic measuring device. The signal from its internal generator was utilized as the input signal for power audio amplifier QSC RMX 1450. Magnets were then powered through a toroidal transformer with ferromagnetic core, immersed in liquid nitrogen as well. In this way the change of the impedance of the secondary due to its heating was excluded. This was important for the phase setting magnet current I_{m} with respect to which the loss part of the measured voltage was acquired. The current of the magnets was measured by the Rogowski coil connected to input channel A of the lock-in. Channel B was utilized for measurement of the voltage signal U_{as} of the anti-serial combination of the measurement and the compensation coil.

Dimensions of both the AC field magnet and the compensation magnet were designed for measurement of the AC magnetization loss of long (up to 10 cm) superconducting tapes—figure 3. Magnets of the race-track shape, using 22 turns in two layers, were constructed from a Cu cable ($1 + 6 \times 0.265$ mm) to suppress eddy current losses. The central wire was used as the measurement coil—in the case of the AC field magnet—and the compensation coil—in the case of the compensation magnet—respectively. In this way, the same dimensions of the magnets and measuring/compensation coils were guaranteed. Dimensions of the magnet bore were 140 mm $\times$ 22 mm. The winding height was chosen to 23 mm to ensure the homogeneity of generated magnetic field. In the central plane, deviation less than 1.5% in the $\pm$1.5 mm width from the longitudinal axis has been achieved. At the frequency $f = 72$ Hz, magnetic field of 12 mT is reached at magnet current $I_{\mathrm{m}} = 10$ A. Attention was dedicated to the proper fixing of the magnet windings, otherwise huge unacceptable disturbing noise can occur due to losses generated by mechanical vibrations. In our case the windings were fixed by wax. During measurement the compensation coil should not feel the sample situated in the measurement coil, otherwise part of the sample loss signal could be subtracted, resulting in an incorrect result. This obstacle can be overcome by placing the AC field magnet and

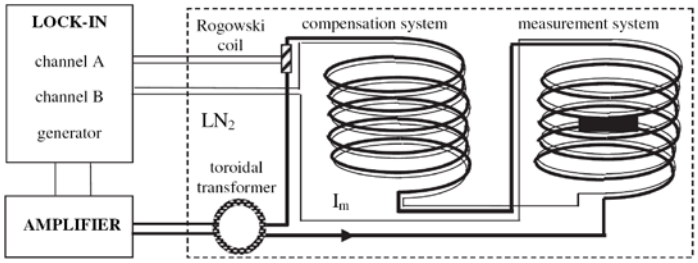

Figure 2. Measurement scheme allowing us to determine the AC loss according to the proposed method.

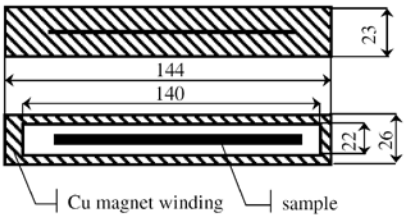

Figure 3. Construction of the AC field magnet (the same dimensions are valid for the compensation magnet). The magnet was constructed from Cu cable ($1 + 6 \times 0.265$ mm) using 22 turns in two layers. Dimensions in the figure are in millimetres. The sample position is shown as well for illustration (not to scale).

compensation magnet at some distance. In our experiments the distance of these magnets was 10 cm and was found to be sufficient for this purpose.

The two systems of AC magnets and coils have been supposed to be identical. In reality, we observed a small signal remaining after the subtraction of the compensation coil signal from that taken from the measurement coil. This could be greatly reduced by the use of an additional compensation (not shown in the principal measurement set-up in figure 2) producing an adjustable inductive signal, which does not influence the loss part of the measured voltage. This additional compensation was realized by utilizing the Rogowski coil signal adjusted by a wide band operational amplifier to the desired value. Using appropriate additional compensation the typical superconducting response can be acquired, as will be shown in the next section.

3. Results and discussion

To confirm the applicability of the described calibration free measurement method, the loss of a loop from Cu wire with known properties was measured at the temperature of 77 K and AC field frequency of 72 Hz. The shape of the loop was rectangular (100 mm $\times$ 4 mm); the wire diameter was $\phi = 0.55$ mm. The resistance of this wire was measured in LN_2 by the four-point DC method. The resistivity was found to be equal to 2.76×10^{-9} Ω m, and the resistance R_{Cu} of the loop in LN_2 was determined to be $R_{Cu} = 2.350$ mΩ.

The Cu loop was placed in the magnet bore, with AC field perpendicular to the loop plane. The phase reference of the lock-in amplifier was set with respect to the magnet current. Two voltage taps have been provided on the straight section of the loop. This allowed us to estimate the current circulating in the loop, I_{Cu}, from the measured voltage and the known resistance of the loop portion between taps. From the loop properties, the ratio between the inductive part and the resistive part of the measured signal was estimated to be less than 10^{-2}. Then the error in such a determination of the I_{Cu} due to self-inductance of the loop was estimated to be lower than 1.5%. At any value of AC field (given by the value of the magnet current I_m), the loss in the Cu loop was determined as

$$P_{cal} = R_{Cu} \times I_{Cu}^2(I_m).$$

The result is to be compared with that obtained with the help of the method proposed here. Again, the phase reference was set with respect to the AC magnet current. The real part of the voltage signal from anti-serially connected measurement and compensation coils $\mathrm{Re}(U_{as\ loop})$ is then the component in phase with the magnet current. The loss of the sample was evaluated using this absolute method as

$$P_{abs} = \mathrm{Re}(U_{as\ loop}) \times I_m.$$

To improve the measurement precision, the background signal $\mathrm{Re}(U_{as\ background})$ was registered first, leaving empty both the measurement and the compensation coils. The corresponding loss value $P_{background}$ evaluated as $\mathrm{Re}(U_{as\ background}) \times I_m$ stretched between 1 and 30 μW at AC field magnet currents I_m in the 1–10 A range.

In figure 4, the dependences of P_{cal} and P_{abs} on magnet current are compared. Utilizing the correction on background signal, coincidence within a few per cent was achieved, confirming the applicability of the suggested method for AC loss measurement.

In the same figure, the AC magnetization loss, $P_{sc\ tape}$, of a 9 cm long superconducting tape[3] measured with the suggested method is shown. Because of the higher level of loss (compared to the Cu loop) the correction on the background signal was negligible. This illustrates sufficient sensitivity of the used apparatus and means that the background correction can be neglected for standard measurements of the superconductors of similar length.

During the measurement of AC magnetization losses of the superconducting tape, the shape of the measured signal $U_{as\ tape}$ was monitored with an oscilloscope. According to the previous considerations, this signal should reflect the superconductor's response to the applied AC field. Indeed, the waveform of a typical superconductor response is acquired as shown in the inset of figure 4. It was taken at $I_m = 5$ A and demonstrates the sensitivity of the apparatus as well.

[3] Australian Superconductor (tape No 2001-3-A/MF).

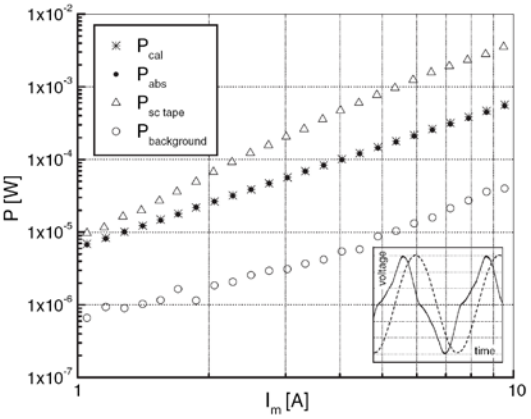

Figure 4. Dependence of the losses on magnet current I_m, P_{cal}—loss of the Cu loop determined as $R_{Cu} \times I_{Cu}^2(I_m)$, P_{abs}—loss of the Cu loop evaluated by the proposed method as $P_{abs} = \mathrm{Re}(U_{as\ loop}) \times I_m$, $P_{sc\ tape}$—loss of the superconducting tape measured by the proposed method, $P_{background}$—background loss measured with empty AC field magnet. Inset: waveform of the signal registered with superconducting tape placed in the AC magnet. Dashed curve—current in the AC magnet, full curve—voltage signal measured on anti-serially connected compensation and measurement coil.

Further work will be devoted to the increasing of the measurement reproducibility and sensitivity with the possibility of measuring smaller AC loss values (e.g. shorter superconducting samples).

4. Conclusion

The new calibration free measuring method was suggested and experimentally verified for the measurement of AC magnetization loss of a superconducting sample exposed to the AC magnetic field. A particular feature of the method is that it does not utilize the traditional pick-up coil. Instead, the loss signal is obtained from the measurement coil whose winding is as far as possible identical with the AC magnet, but without any galvanic contact to the magnet. A parallel winding of the AC magnet and the measurement coil could serve well for this purpose. To achieve practical feasibility of the method, two identical magnetic systems, each containing an AC magnet and a measurement coil, are first balanced to give zero total signal. Subsequently, when the sample is placed in one of the AC magnets, the voltage appears on the anti-serial connection of two measurement coils. This signal is a direct measure of the power supplied by the AC source to cover the AC loss in the sample. Therefore, no measurement and/or calculation of the calibration constant is required. Moreover, the kind and the shape of the sample do not play any role in the loss evaluation.

Acknowledgments

The authors would like to thank J Tančár for his helpful technical assistance. This work has been partially supported by the Grant Agency VEGA (contract 2/3117/23) and the Science and Technology Assistance Agency (contract APVT-20-012902).

References

[1] Chen D X, Pardo E, Navau C, Sanchez A, Fang J, Zhu Q, Luo X M and Han Z H 2005 *Supercond. Sci. Technol.* **17** 1477–84

[2] Rillo C, Lera F, Badía A, Angurel L A, Bartolomé J, Palacio F, Navarro R and van Duynaveldt A J 1991 *Proc. Office of Naval Research Workshop on Magnetic Susceptibility of Superconductors and Other Spin Systems (Coolfont, Berkeley Springs, West Virginia, May 1991)* ed R A Hein, T L Francavilla and D H Liebenberg, p 1

[3] Goldfarb R B, Lelental M and Thompson C A 1991 *Proc. Office of Naval Research Workshop on Magnetic Susceptibility of Superconductors and Other Spin Systems (Coolfont, Berkeley Springs, West Virginia, May 1991)* ed R A Hein, T L Francavilla and D H Liebenberg p 49

[4] Jiang Z and Amemiya N 2004 *Supercond. Sci. Technol.* **17** 371–9

[5] Jiang Z, Amemiya N, Ayai N and Hayashi K 2004 *Supercond. Sci. Technol.* **17** 314–21

[6] Rabbers J J, van der Meer O, Zeggeling W F A K, Shevchenko O A and ten Haken B 1999 *Physica* C **325** 1–7

[7] Rabbers J J 2001 *PhD Thesis* Low Temperature Division of the Department of Applied Physics, University of Twente, Enschede, The Netherlands

[8] Rabbers J J, ten Haken B and ten Kate H H J 2001 *Rev. Sci. Instrum.* **72** 2365–73

[9] Couach M and Khoder A F 1991 *Proc. Office of Naval Research Workshop on Magnetic Susceptibility of Superconductors and Other Spin Systems (Coolfont, Berkeley Springs, West Virginia, May 1991)* ed R A Hein, T L Francavilla and D H Liebenberg, p 25

[10] Yang Y, Hughes T J, Beduz C and Darmann F 1998 *Physica* C **310** 147–53

[11] Iwakuma M, Nanri M, Fukui M, Fukuda Y, Kajikawa K and Funaki K 2003 *Supercond. Sci. Technol.* **16** 545–56

[12] Martínez E, Yang Y, Beduz C and Huang Y B 2000 *Physica* C **331** 216–26

[13] Yang Y, Martínez E and Norris W T 2004 *J. Appl. Phys.* **96** 2141–9

[14] European Standard EN 61788-8 2003 *Superconductivity, Part 8: AC Loss measurements—Total AC Loss Measurement of Cu/Nb-Ti Composite Superconducting Wires Exposed to a Transverse Alternating Magnetic Field by a Pickup Coil Method*

[15] Oomen M P, Rieger J, Leghissa M and ten Kate H H J 1997 *Physica* C **290** 281–90

[16] Amemiya N, Jin F, Jiang Z, Shirai S, ten Haken B, Rabbers J J, Ayai N and Hayashi K 2003 *Supercond. Sci. Technol.* **16** 314–21

[17] Ashworth S P and Suenaga M 1999 *Physica* C **313** 175–87

Experiment Setup for Calorimetric Measurements of Losses in HTS Coils due to AC Current and External Magnetic Fields

John P. Murphy[1], Matthew J. Mullins[2], Paul N. Barnes[2], Timothy J. Haugan[2], George A. Levin[3], Milan Majoros[4], Michael D. Sumption[4], Edward W. Collings[4], Milan Polak[5], and Pavol Mazola[5]

***Abstract*--We present a design and details of construction of two calorimetric systems that allow us to measure the total loss in high temperature superconducting coils or linear samples carrying alternating current while exposed to a strong alternating magnetic field. This measurement technique is based on the boil-off of liquid nitrogen. A distinguishing characteristic of the protocol of our measurements is that the electric current is turned on only for a relatively short period of time, so that the system does not achieve the steady state boiling. This limits the temperature rise of the sample, allowing us to determine the losses while keeping the temperature of the sample close to 77 K. The sensitivity of the system is such that it can measure low losses from a few mW to several hundred mW, in either a static or dynamic magnetic field.**

Index Terms—***AC Losses, calorimetric measurement, magnetic field.***

I. Introduction

As $YBa_2Cu_3O_{7-x}$ (YBCO) coated conductors can now be made in substantial lengths [1], they have become of interest for use in various devices, including field windings in motors and generators [2], transformers [3], and superconductor magnet energy storage devices [4], in addition to the power transmission cables [5], which was the initial goal in their early development. A critical characteristic of wires and cables for many of these applications is their AC losses. The need to measure these losses in device relevant environments have led to the development of several techniques. Some infer the losses through electromagnetic measurements [6,7], others use calorimetric methods based on the measurement of the temperature increase of the sample [8,9] or the rate of cryogen boil-off [10]. All these methods have their strengths and weaknesses and for particular experimental conditions some are more suitable than others.

In this paper we briefly describe two systems developed for measurements of the total AC losses in HTS samples and coils. The first system was developed as a sensitive LN_2 boil off calorimeter which allows us to measure the self-field losses caused by a transport AC current. A coil is placed in liquid nitrogen and the losses caused by ac current are determined from the total amount of evaporated nitrogen. The specific of our approach is that the AC current is turned on for a short period of time (a few minutes), so that over this "active" period the steady state boiling regime is not achieved and the temperature of the coil is not raised significantly.

The second system, a larger machine, designed with a long term prospective to serve a test bed for the novel types of superconducting wires and coil concepts for many years to come. This machine consists of an eight-pole rotating magnet and the position of the test coil or a straight sample is similar to that they would have in the armature winding of a motor or generator. In the previous experiments on ac losses where the time-varying magnetic field was generated by a solenoid, the maximum sweep rate *Bf* did not exceed 15 - 20 T/s [11-16]. At the early stage of this project we have come to conclusion that the effort to build a new machine can be justified only if its potential exceeds by at least an order of magnitude the parameters that had been achieved previously. Also, the generators currently used on airborne platforms operate at a frequency of 400 Hz. This was an additional consideration influencing the design parameters. The ac losses in this system are also measured by a sensitive boil-off calorimeter.

II. Self-field System

The self-field system shown in Fig. 1 used an outer cryostat consisting of a LHe dewar with a LN_2 thermal radiation shield. The removable sample chamber was fabricated from a G-10 fiberglass tube bonded to an aluminum flange to fit the 12.7

Manuscript submitted October 9 2012. This work was supported by the Air Force Research Laboratory, through the Power Generation Division (RZPG) under contract _____

J. P. Murphy is with the University of Dayton Research Institute, Dayton, OH 45469-0073 USA (e-mail: john.murphy.ctr@wpafb.af.mil)

M. J. Mullins was a Mechanical Engineering grad student working with the Air Force Research Laboratory (e-mail: manaman22@gmail.com)

P. N. Barnes is Chief of Power Components in the Energy and Power Division, Sensors and Electron Devices Directorate, Army Research Laboratory, Adelphi, MD 20783 USA (e-mail: paul.n.barnes.civ@mail.mil)

T. J. Haugan is with Aerospace Systems Directorate of The Air Force Research Laboratory, Wright-Patterson AFB, 45433 USA (email: timothy.haugan@wpafb.af.mil)

G. A. Levin is with UES, Dayton, OH 45432 USA (e-mail: george.levin.ctr@wpafb.af.mil)

M. Majoros is with the Ohio State University, Columbus OH 43210 (email: majoros@matsceng.ohio-state.edu

M. D. Sumption is with the Ohio State University, Columbus OH 43210 (email: sumption@matsceng.ohio-state.edu

E. W. Collings is with the Ohio State University, Columbus OH 43210 (email: collings@ecr6.ohio-state.edu

M. Polak is with the Slovak Academy of Sciences, 84104 Bratislava, Slovakia (email: milan.polak@savba.sk)

P. Mazola with the Slovak Academy of Sciences 84104 Bratislava, Slovakia (email: pavol.mazola@savba.sk)

cm diameter opening for the original LTS magnet. In this flange LN_2 fill and vent ports, a sampling port, and the 7.6 cm diameter opening for power leads cooling section were cut.

The current leads were two 75 cm lengths of 6 gauge copper braid passing through a 1 m vertical length of 7.5 cm OD PVC pipe filled with LN_2 for heat removal, feeding a 10 cm diameter by 13 cm tall sample space.

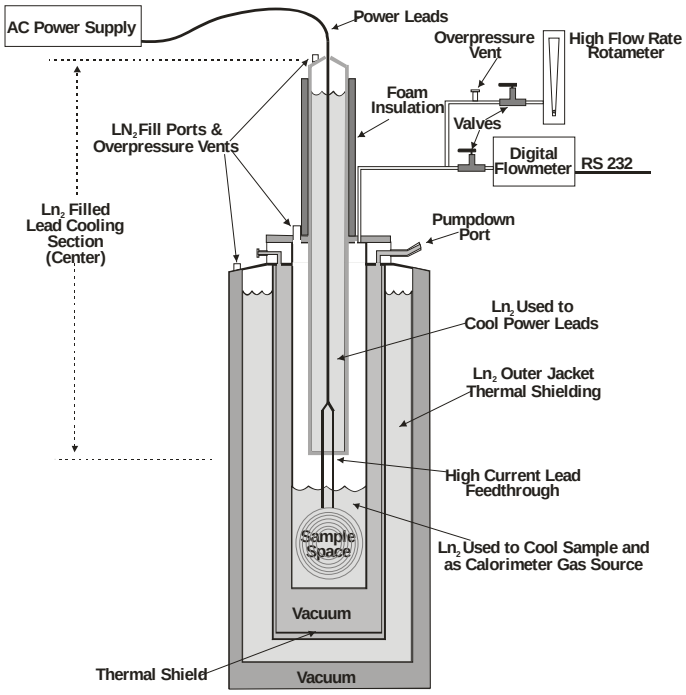

Fig. 1. Vertical cross section of self field cryogenic calorimeter

Altogether this makes a series of five concentric cylindrical enclosures that include the lead cooling section, the sample chamber surrounded by deep vacuum insulation, the LN_2 thermal radiation shield and the outer aluminized Mylar wrapped evacuated insulation space as shown in Fig. 1.

An important feature of this design that sets it apart from many other cryogenic calorimeters, e. g**.** Refs. [10,17, 18], is that the sample chamber and the current leads cooling section do not share the same pool of LN_2, and the sample chamber is sealed from the environment and from the current leads cooling section. This significantly reduces changes, as well as the magnitude, in the base flow rate of evaporation.

A. Protocol of operation and experiments

The flow rate was calibrated using resistance heaters. A thin film heater of 50 Ω resistance was sandwiched between two aluminum plates in order to increase the surface area and avoid the film boiling. It was placed in close proximity to the tested HTS coil.

Since the coil is usually enclosed in the epoxy shell, it was virtually impossible to obtain reliable data by waiting until the outflow of evaporated nitrogen stabilizes. The temperature of the superconducting material by that time could not be determined, and it would vary with the magnitude of the transport current.

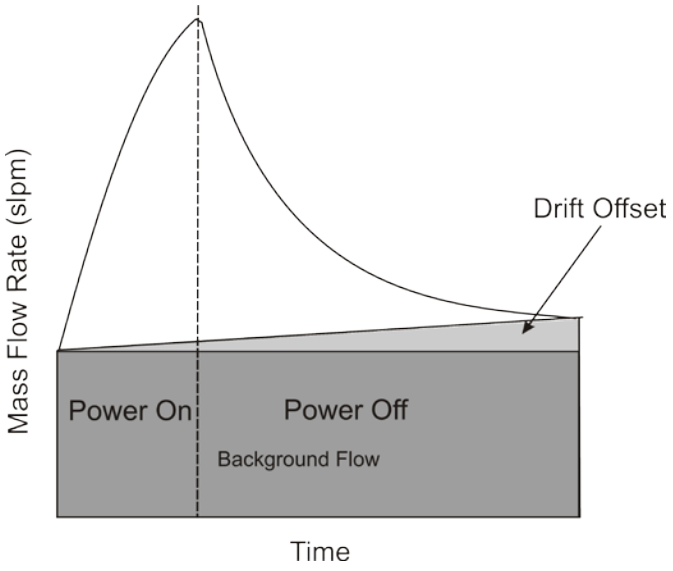

Figure 2. Time dependence of the mass flow signal.

We have used a measurement protocol illustrated in Fig. 2. The current through the coil that generates losses was turned on for about three minutes. Over this period of time the outflow of gas increases. When the current is turned off, the mass flow gradually decreases reaching the background level. Thus, knowing the total amount of evaporated nitrogen above the background level, and correcting for background flow drift, we can calculate the total excess of energy deposited into the pool of LN_2 by the coil. Dividing this energy by the time the current was running, we obtain the power loss. Our estimates based on heat capacity of the coil indicate that the maximum temperature rise inside the coil was of the order of 1 K or less.

The ohmic power loss in the current contacts was determined by running dc current through the coil. This amount was subtracted from the total loss. We have found by trial an alternative way of determining losses. In experiments with the heater, the rate of increase of the outflow of gas (the initial slope in Fig. 2) was directly proportional to the power deposited through the heater. This allows us to determine the power loss by using the gas flow data accumulated within first 90 s. The advantage of this method is that there is no need to account for changes in the background rate over the period of 10-20 minutes, which is a characteristic time constant of this apparatus, Fig. 2.

The precision of the aforementioned methods of determining ac loss were verified by carrying out the measurements on a coil that was previously used to determine the ac loss by electromagnetic measurements [7]. We were satisfied that the results obtained by calorimetric methods were in good agreement with these results.

III. ROTATING MAGNETS MACHINE

The second system, shown in Fig. 3, for measuring ac losses consists of an eight-pole permanent magnet rotor. Fig. 4 shows schematically the structure of the machine. The central shaft carries the rotating NdFeB magnet Hallbach array (30 cm OD), surrounded by 3.8 cm of annular vacuum space (a place

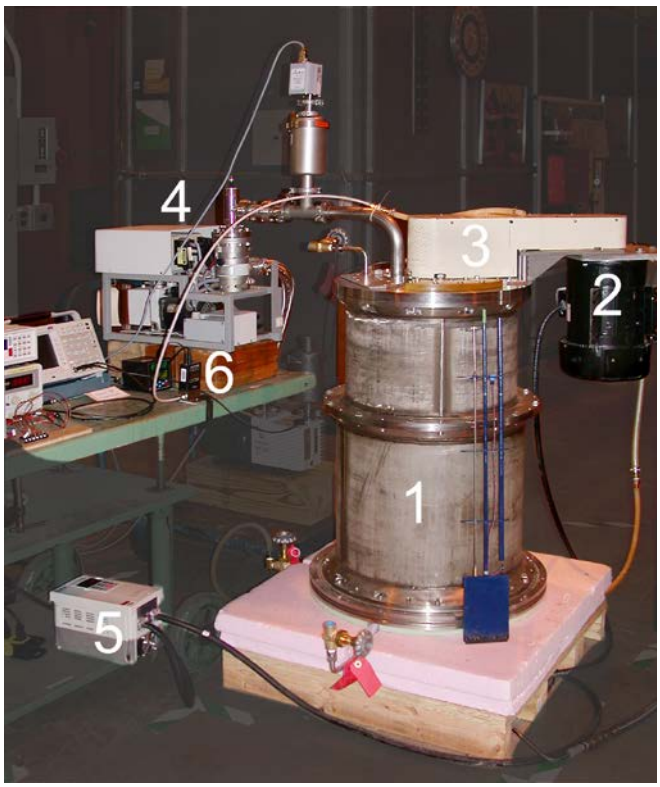

Fig. 3 Photograph of assembled system showing the evacuated main vessel containing the magnet rotor (1). Also shown is the drive motor (2), drive belt (3), vacuum pump (4), Drive motor control (5) and flow meter (6).

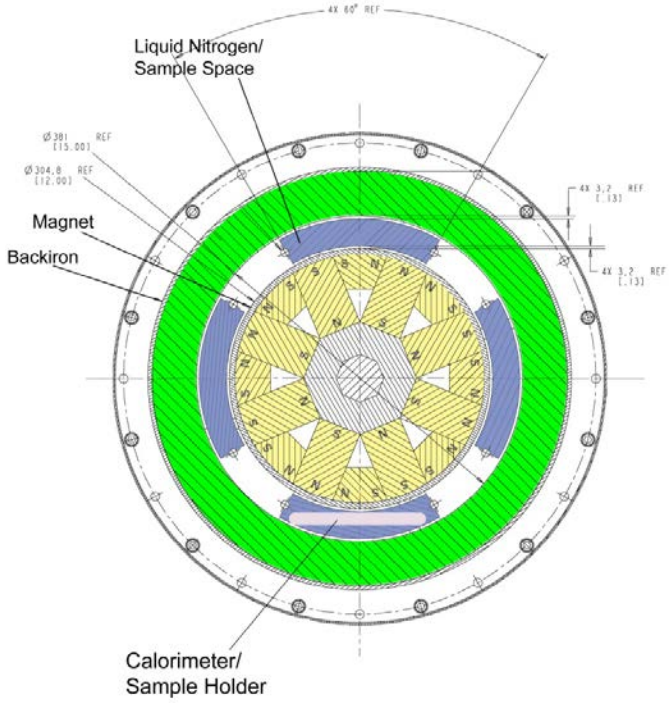

Fig. 4. Cross section of the rotating magnets machine. Shown are eight-pole rotor assembly (maintained at room temperature), four sample chambers inside the vacuum gap, LN_2 – cooled sample holder (currently only one is in use), the laminated back iron, and the outer shell.

where armature winding would be in a generator or motor). This gap contains the sample chambers in which a cryostat sample holder (shown at the bottom of Fig 4) can be inserted. The size and shape of the sample chamber and sample holder

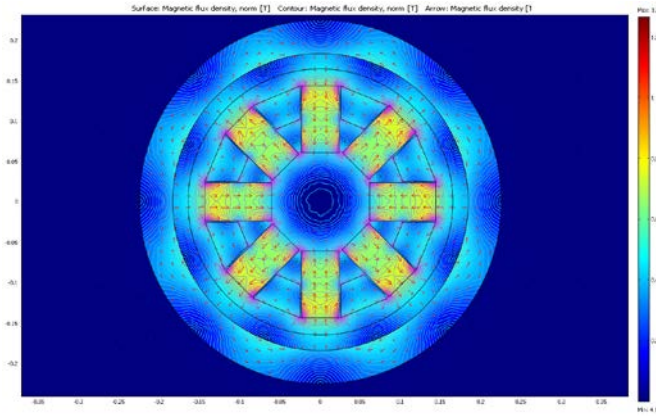

Fig. 5. Color map of the field strength inside the machine.

accommodate a variety of different small coils and linear tapes. This assembly is surrounded by the laminated back iron and the outer shell that seals the vacuum. Maintaining vacuum inside the machine minimizes the heat leaks into the cryostat holder containing samples.

This machine was built with the goal to closely simulate the stator environment in a motor or generator, so that the superconducting samples and coils can be tested in the environment characteristic of the stator windings. The rotating magnet was designed for maximum speed of 6000 rpm, which the eight-pole rotor translates into 400 Hz frequency of the magnetic field (a typical frequency of aircraft based generators).

The spatial profile of the magnetic field strength in the vacuum gap of the fully assembled system was mapped while the magnets were rotating using a 1 cm, ten turn copper wire coil. The measured values of the field correlated well with the finite elements calculations shown in Fig. 5.

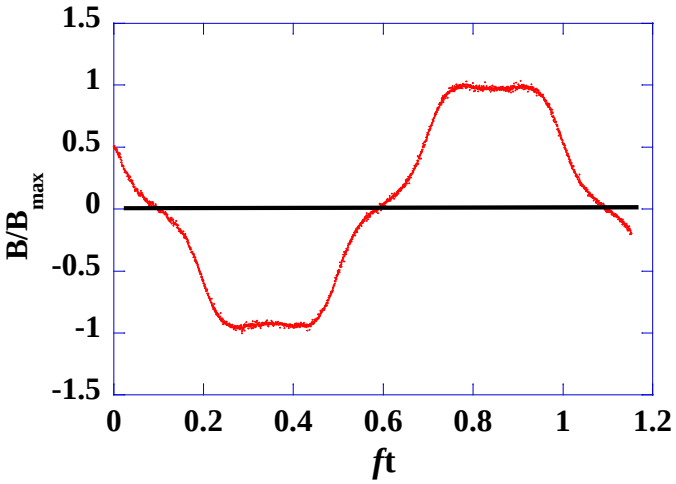

Fig. 6. Time dependence of the magnetic field at a given point inside the sample chamber. Approximately one cycle is shown. The field is normalized to its maximum value at a given point.

The maximum radial component of the magnetic field in the sample holder is 0.5 T. At the maximum rotation speed this would expose the sample located in this area to 200 T/s sweep rate, which is about an order of magnitude greater than the maximum sweep rate that has been achieved in ac solenoids. It should be noted that the machine has not yet been run at the

maximum speed. It has been tested so far only at 900 - 1200 rpm (60 – 80 Hz).

Fig. 6 shows the time dependence of the radial component of the magnetic field in the center of the sample chamber. The flat top shape is characteristic of most rotating machines and is characterized by the presence of high frequency harmonics.

A. *Operation and Experiments*

The first sample holder for this machine was constructed to hold 10 cm long sections of HTS tape or a coil, up to 10 cm in diameter, made out of 4 mm wide conductor. This sample holder has a sealed volume 10x10x 0.5 cm^3 with a valved fill port and a gas collection port. It contains two resistors to determine the internal LN_2 level and a third, 100 ohm resistor for calibration. To determine the boil off rates resulted from ac losses we have used 10 x 5 x 0.05 cm^3 copper strip that generates eddy current losses in rotating field. The copper strip was used to develop the operating procedure and to carry out the reproducibility tests.

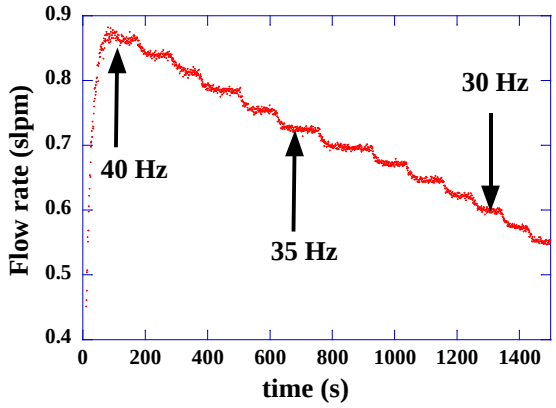

Fig. 7. Flow rate in standard liters per minute due to eddy current losses in a copper strip. The rotation frequency of the rotor decreases in steps. The arrows show the frequency of field variation at a given moment.

Fig 7 shows a representative example of the changes in flow rate from the sample holder containing the copper strip in response to changing rotation speed of the rotor. The initial speed is 600 rpm, which corresponds to the field variation frequency 40 Hz. The rotation speed was reduced over time in steps of 15 rpm (1 Hz) and the outflow decreased in corresponding steps.

IV. CONCLUSIONS

Two AC loss measurement systems were designed, built and initially tested. The first system provides for the measurement of ac losses in coils due to an applied ac current. This self-field system has a resolution of about 10 mW and a minimum flow rate corresponding to power loss of 20 mw. The second system determines ac losses in the presence of rotating magnetic field with the sweep rate, as currently tested, up to 30-40 T/s, and with the potential to reach 150-200 T/s with the maximum frequency of the rotating field up to 400 Hz. Initial calibration and test results are described.

REFERENCES

[1] V. Selvamanickam et al. IEEE Trans. on Appl. Supercond. 21, 3049 (2011)

[2] P. N. Barnes, M. D. Sumption, G. L. Rhoads, Review of high power density superconducting generators: Present state and prospects for incorporating YBCO windings. *Cryogenics* 45 (2005) 670–686

[3] M. Yamamoto, M. Yamaguchi, K. Kaiho, Superconducting Transformers. *IEEE Transactions on Power Delivery, Vol. 15, No. 2, April 2000*

[4] A. Ishiyama, H. Ueda, Y. Aoki, K. Shikimachi, N. Hirano, and S. Nagaya, Quench Behavior and Protection in Cryocooler-Cooled YBCO Pancake Coil for SMES *IEEE Transactions on Applied Superconductivity*, Vol. 21, No. 3, June 2011

[5] C. Træholt, E. Veje, O. Tønnesen, Electromagnetic losses in a three-phase high temperature superconducting cable determined by calorimetric measurements. *Physica C 372–376 (2002) 1564–1566*

[6] G. Coletta, L. Gherardi, **F.** Giimiiry, E. Cereda, V. Ottoboni, D. Daney, M. Maley, **S.** Zannella. Application of Electrical and Calorimetric Methods to the AC Loss Characterization of Cable Conductors *IEEE Transactions on Applied Superconductivity*, Vol. 9, No. 2, June 1999.

[7] Polak, M., et al. AC Losses in a YBa2Cu3O7-x Coil. Applied Physics Letters 88 (2006).

[8] S P Ashworth, M Suenaga Local Calorimetry to Measure AC Losses in HTS Conductors. *Cryogenics* 41 (2001) 77-89

[9] P. Ghoshal, T. Coombs, A. Campbell. Calorimetric method of ac loss measurement in a rotating magnetic field. *Review of Scientific Instruments* **81**, 074702 (2010)

[10] F. Darmann, S. Dou, C. Cook, Determination of the AC Losses of Bi-2223 HTS Coils at 77 K at Power Frequencies Using a Mass Boil-Off Calorimetric Technique *IEEE Transactions on Applied Superconductivity*, Vol. 13, No. 1, March 2003.

[11] N. Amemiya, S. Kasai, K.Yoda, Z. Jiang, G. A. Levin, P. N. Barnes, and C. E. Oberly, Supercond. Sci. Technol. 17, 1464 (2004).

[12] M.D. Sumption, E.W. Collings, and P.N. Barnes, Supercond Sci. Technol., **18**, 122-134 (2005).

[13] M. Majoros, B. A. Glowacki, A. M. Campbell, G. A. Levin, P. N. Barnes, and M. Polak, *IEEE Trans. Appl. Supercond.*, vol. 15, p. 2819, (2005.

[14] G. A. Levin, P. N. Barnes, N. Amemiya, S. Kasai, K. Yoda, Z. Jiang, and A. Polyanskii, *J. Appl. Phys.*, 98, 113909, 2005

[15] P. N. Barnes, G. A. Levin, C. Varanasi, and M. D. Sumption, IEEE Trans. Appl. Supercond. 15, 2827 (2005).

[16] G. A. Levin, P. N. Barnes, J. W. Kell, N. Amemiya, Z. Jiang, K. Yoda, and F. Kimura, Appl. Phys. Lett. **89**, 012506 (2006)

[17] N Magnusson, S Hornfeldt, JJ Rabbers, B ten Haken, HHJ ten Kate. Comparison Between Calorimetric and Electromagnetic Total AC Loss Measurement on a BSCCO/Ag Tape. *Supercond. Sci. Technol.* **13** (2000) 291-294

[18] S. Bernd, Handbook of Applied Superconductivity. *Institute of Physics Publishing*, 1998 Pg 347

AC Losses of Copper Stabilized Multifilament YBCO Coated Conductors

G. A. Levin[1,2], J. Murphy[1,3], T. J. Haugan[1], J. Šouc[4], J. Kováč[4], and P. Kováč[4]

***Abstract* — We report the data on magnetization losses and critical current of multifilament copper stabilized coated conductors. Eight centimeters long samples of copper stabilized $YBa_2Cu_3O_{7-x}$ (YBCO) coated conductors manufactured commercially were subdivided into superconducting filaments by near-IR laser micromachining. The width of the superconducting stripes was varied from 30 μm to 200 μm. Some of the samples were striated leaving superconducting bridges for current sharing between the filaments. The AC losses were measured at different sweep rates of the magnetic field up to 4 T/s. We will present the results for the hysteresis and coupling losses and discuss the means to reduce the coupling loss by changing the processing parameters of micromachining and by post-ablation treatment. The optimal filament width based on the criterion of minimum loss per unit of critical current will be evaluated as well.**

***Index Terms*—AC loss, coated conductors, striated stabilizer.**

I. Introduction

Over the years there has been a significant effort by several research groups, as well as by the manufacturers of coated conductors, to implement striation as a means to reduce the AC losses in the future power cables. By far an incomplete list of such publications includes references [1-9]. Another interesting, perhaps a niche, application of striated coated conductors is integration on the same substrate of multiple mini-current leads to feed the cryo-electronics [10]. For both of these purposes (AC power cables and current leads) the stabilization of the superconducting filaments by copper or silver layer of substantial thickness is necessary to avoid a catastrophic (one that results in irreversible damage) quench. The individual stripes must be well insulated from each other in order to avoid the coupling losses, which may defeat the purpose of striation, and to avoid the cross-talk in current leads. Most early experiments with striated coated conductors were carried out, as a proof of concept, on non-stabilized samples with only a thin (1-3 μm) silver layer on top of YBCO film. Later, some groups went farther, and carried out the striation of coated conductors with a stabilizer applied [8, 11].

Here we present the results of measurements of the critical currents and AC losses in fully stabilized and laser striated coated conductors. The width of the individual stripe was varied from 200 to 40 μm. The thickness of copper stabilizer striated along with the superconducting layer was 20 μm. We have determined the contributions of the hysteresis, coupling and eddy current loss to the total. One of the conclusions we draw from this sequence of experiments is that fine striation, while decreasing the overall critical current, increases the pinning strength which translates into less steep fall of the critical current in magnetic field. While the striation leads to substantial reduction of AC loss per unit of critical current, many stripes remain partially coupled, so that the effective width of the stripe which determines the hysteresis loss is greater than the nominal width of an individual stripe. We also determined that the coupling loss exceeds that of the eddy current loss.

II. Experimental Details

A. Sample preparation

Laser micromachining of coated conductors is a method that has been tested thus far more extensively than its potential alternatives (photolithography, etc.). We have used a frequency tripled diode-pumped solid-state Nd:YVO_4 laser at 355 nm wave length to cut grooves in the 12 mm wide samples of copper stabilized coated conductors produced by SuperPower Inc. The 20 μm thick copper stabilizer layer was wrapped around the whole tape (surround copper stabilizer), but only one side of the stabilizer, which is in contact with the superconducting film, was striated. The back side of the

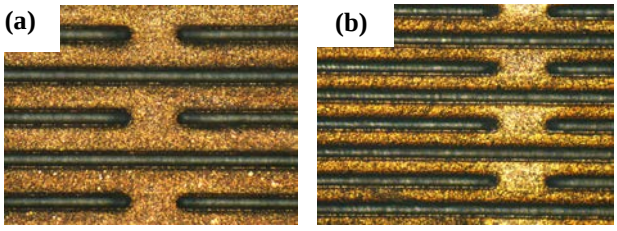

Figure 1(a,b) Striated samples with the laser cut grooves (shown at 10x magnification). The width of the individual stripes is 70 μm in Fig. 1(a) and 40 μm in Fig. 1 (b). Superconducting bridges facilitating current transfer between the individual stripes were left in some samples.

Manuscript received October 9, 2012. This work was supported by the U.S. Air Force Office of Scientific Research and its European Office of Aerospace Research and Development.

G. A. Levin is with UES, Inc. Dayton, OH 45432 USA (937-255- 5630, George.levin.ctr@wpafb.af.mil.

J. Murphy is with the University of Dayton Research Institute, Dayton OH 45469, USA.

T. J. Haugan is with the Aerospace Systems Directorate, Air Force Research Laboratory, Wright-Patterson AFB OH 45433, USA

J. Šouc is with the Institute of Electrical Engineering, Slovak Academy of Sciences, 841 04 Bratislava, Slovakia

J. Kováč is with the Institute of Electrical Engineering, Slovak Academy of Sciences, 841 04 Bratislava, Slovakia

P. Kováč is with the Institute of Electrical Engineering, Slovak Academy of Sciences, 841 04 Bratislava, Slovakia

stabilizer was not striated and had served as an additional source of eddy current losses. In some samples superconducting bridges were left in order to allow the current exchange between the individual stripes as a measure of increasing reliability of the overall conductor [3,5,12,13].

B. *Critical current measurements*

Multiple, parallel 8 cm long grooves were cut in the central section of 12 cm long tapes leaving sufficient unstriated margins at both ends in order to measure the critical current I_c using a standard 4-point method. The voltage criterion for determining I_c was chosen as 1 μV/cm. The measurements were carried out for both directions of the applied current and yield very close results. The magnetic field B was applied perpendicular to the wide face of the tape. The temperature was kept at 77 K by immersing the samples in liquid nitrogen.

C. *AC loss measurements.*

After the critical current was determined, the unstriated ends were cut resulting in 8 cm long fully striated samples for measuring the AC losses. The AC loss measurement method is based on the measurement of a part of the power supplied by the AC source to the AC solenoid generating the magnetic field. The measurement system consists of two identical ac copper solenoids connected in series and two measurement pick-up coils wound in parallel with magnets windings. During the measurements the complete system is immersed in liquid nitrogen. The superconducting sample is located inside one of the solenoids, with the other solenoid and a pick-up coil serving as compensation. More details about the calibration free method for AC loss measurement are described in Ref. [14].

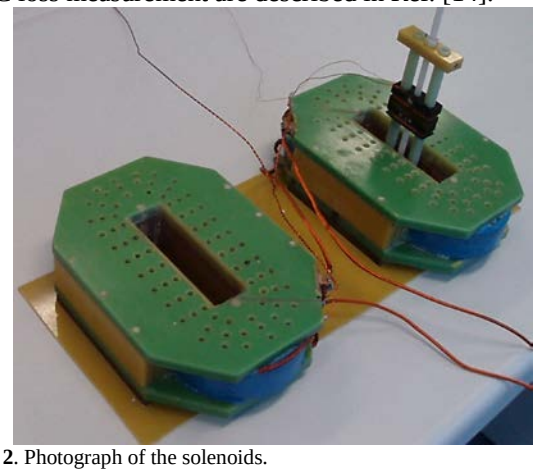

Figure 2. Photograph of the solenoids.

III. RESULTS

A. *Critical current*

Figure 2(a) shows the critical current of several striated samples as a function of magnetic field. As expected, the greater the number of stripes, the smaller the critical current is due to removal of successively larger amount of superconducting material. The width of the non-superconducting grooves is approximately 30 μm. In Fig. 2(b) the critical currents of all samples are normalized to their value at zero field. Here we see that the finely striated

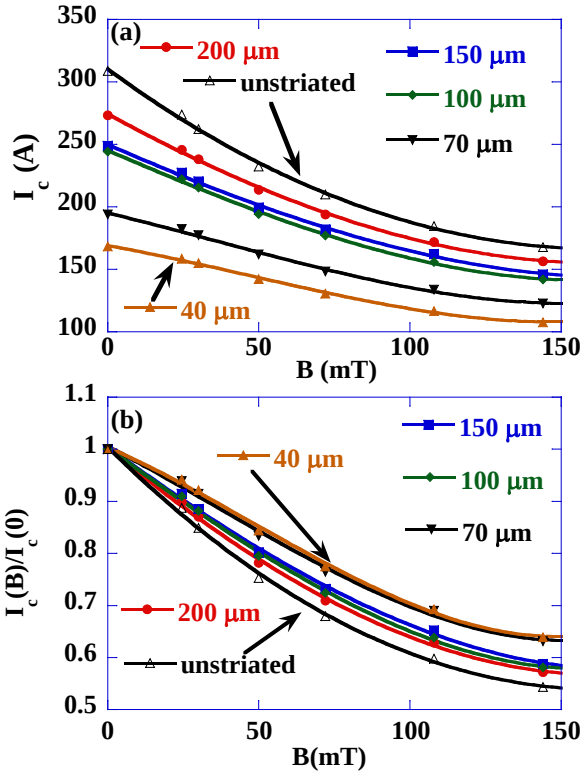

Figure 2(a,b) (a) Measured critical current vs applied magnetic field for several striated and one non-striated sample. The width of the stripes is indicated. (b) The same data as in Fig. 2(a), but the currents are normalized to their values in zero applied field. Arrows indicate the data for non-striated sample and the one with the maximum number of stripes, each 40 μm wide.

samples, especially the ones divided into 40 or 70 μm wide stripes retain the value of the critical current better than the non-striated or more coarsely striated conductors. For example, the critical current of the non-striated sample falls to 50% of its zero field value in field of 150 mT. The sample with 40 μm wide stripes has the critical current equal to 64% of its zero field value in the same field. Of course, nobody would suggest striation as a means to improve the current-carrying capacity of the coated conductors. These results, however, lend additional support to experimental findings and theory considerations advanced in Ref. [15] that the edge-barrier pinning leads to enhanced critical current in field. Although 40 and 70 μm wide stripes seem too wide to have such a pronounced effect, other types of damage caused by laser ablation may have a beneficial side-effect increasing the number and strength of the pinning centers.

B. *AC losses.*

Striated samples like the ones shown in Fig. 1 have three main components of AC loss. One component is the hysteresis loss in superconducting material. In magnetic field above the penetration threshold [16]

$$P_h \approx I_c W_n B f \quad . \qquad (1)$$

Here P_h is the hysteresis loss per unit length, W_n is the width of an individual stripe and Bf is the sweep rate, where B is the peak value of the alternating field and f is its frequency.

Sweep rate characterizes the average value of the time derivative $|\dot{B}| \propto Bf$. The eddy current loss in these samples is predominantly originates from the back side of the stabilizer, which is left unstriated. The eddy current loss per unit length in a rectangular tape is given by [17,18]

$$P_{e-c} \approx \frac{\pi^2}{6}\frac{dW^3}{\rho}(Bf)^2 \cdot \qquad (2)$$

Here d is the thickness of the metal stripe, W is its width, and ρ is the resistivity. The third component of ac loss originates from the remaining resistive coupling between the superconducting stripes and is also proportional to the square of the sweep rate. By analogy with Eq. (2) we can write down a phenomenological expression for the coupling losses [5,19,20] as

$$P_c \approx \frac{\pi^2}{6}\frac{L^2 W}{R_{eff}}(Bf)^2 \cdot \qquad (3)$$

Here the effective resistance R_{eff} characterizes the coupling strength. The total ac loss [W/m]

$$P = P_h + P_c + P_{e-c} \qquad (4)$$

can be presented in the form of the power loss per unit length, per unit of the sweep rate, per unit of the critical current as a function of the sweep rate

$$\Lambda \equiv \frac{P}{I_c Bf} = \lambda_1 + \lambda_2 (Bf) \qquad \text{[m]}. \qquad (5)$$

This allows us to segregate the hysteresis loss from the eddy current and coupling losses as the intercept λ_1 and the slope λ_2 [5,20]. If the striation is carried out perfectly, so that there is no superconducting links between the stripes, and the critical current is not degraded beyond the loss of superconducting material, the value of the intercept will be close to the width of the stripes, see Eq. (1), as indeed was the case in the striated samples without stabilizers [5,20]. However, if the intercept λ_1 is substantially greater than W_n, it is an indication of remaining superconducting connections between the stripes, or a more serious degradation of the critical current (by overheating and loss of oxygen, for example, during striation).

C. Control experiment.

As a control experiment we used a coated conductor covered only with a thin silver layer. The 12 mm wide sample was striated into 500 μm wide stripes, its critical current and AC losses were measured as described above. Figure 3 shows the power loss presented in the form of Eq. (5) as the power loss per unit length, per unit of the sweep rate, per unit of the critical current. The linear fit shown in the Figure gives us the values of the intercept and the slope. The intercept exactly matches the width of the individual stripes indicating a perfect striation (absence of superconducting connections between the stripes). The slope indicates substantial coupling loss due to normal metal coupling between the stripes. The value of the slope shown in the Figure is that obtained by a fit to 72 Hz data. The reason why the two slopes (72 Hz and 36 Hz data) are different is not clear and may be attributed to experimental errors or to the changes in the properties of the sample taken

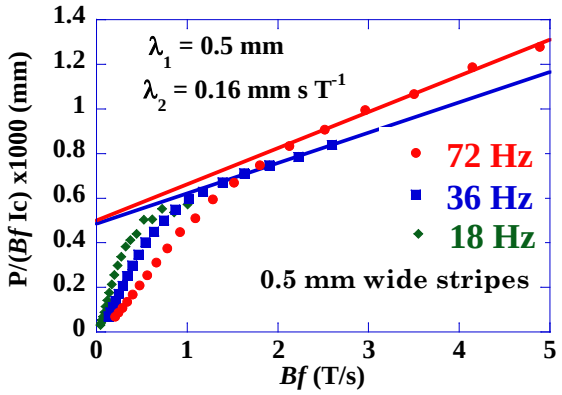

Figure 3. Power loss per unit length, per unit of the sweep rate, per unit of the critical current, Eq. (5). The critical current I_c = 217.6 A. The intercept λ_1=0.5 mm and the slope λ_2 are the measures of the hysteresis loss and coupling loss, respectively. The straight lines correspond to the linear fit of 72 and 36 Hz data.

place between the measurements. The results shown in Fig. 3 are similar to those obtained earlier on similar samples [5,20].

The value of the slope determines the sum of the coupling and eddy current losses. The contribution of the eddy current losses to the slope is given by Eq. (2):

$$\lambda_2^{e-c} = \frac{\pi^2}{6}\frac{dW^3}{\rho I_c} \quad . \qquad (6)$$

In this sample the eddy current losses are determined by the 50 μm thick Hastelloy substrate with the resistivity $\rho \approx 120\times10^{-6}\Omega cm$. Taking W=12 mm and I_c=217.6 A, we get

$$\lambda_2^{e-c} \approx 5.4\times10^{-4} mm\cdot s\cdot T^{-1}. \qquad (7)$$

Comparing this with the total value of λ_2= *0.16 mm s* T^{-1} shown in Fig. 3 we conclude that the main contribution to the loss with quadratic dependence on the sweep rate is the coupling loss originated from the metal connections between the stripes. When the striated sample was later annealed in oxygen, the coupling component of the total loss disappeared, because metal oxides that has formed in the grooves insulated the superconducting stripes from each other [21,22].

D. Losses in striated and copper stabilized samples.

Figure 4 shows the ac losses presented in the form of Eq. (5) in the copper stabilized sample for two different frequencies of the applied magnetic field. The data for both frequencies strongly overlap, confirming the universality of the description given by Eq. (5). The value of the critical current was that measured in zero applied field, Fig. 2(a).

The sample is divided into approximately 50 stripes, 200 μm wide each with approximately 30 μm wide grooves segregating them. The intercept λ_1=1.2 mm is significantly greater than the expected value λ_1=0.2 mm. There are two possible reasons for that. One possibility is that there is significant superconducting coupling between the stripes. In the absence of such connections, the intercept would be close

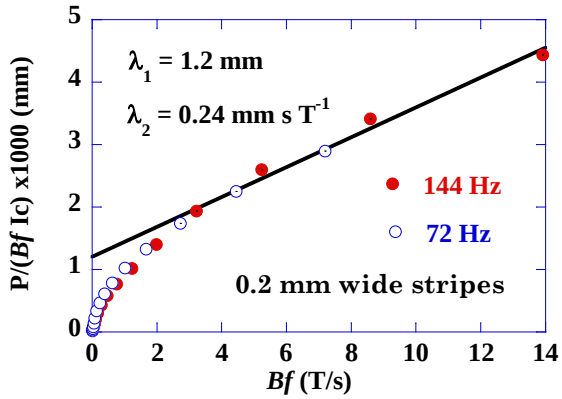

Figure 4. AC power losses in the form of Eq. (5) in the sample with 200 μm wide stripes for two different frequencies 77 and 144 Hz. The grooves segregating the stripes were cut through the 20 μm thick stabilizer and YBCO film. The critical current I_c=273 A. The line is a linear fit to the data which includes both frequencies.

to 0.2 mm, equal to the width of the stripe (see Fig. 3). The hysteresis loss per unit of critical current in this 50 stripe sample is equivalent to that in a perfectly striated sample with 10 stripes, each 1.2 mm wide. The superconducting connections between the stripes are likely formed by a random network of microscopically small superconducting links that have survived the laser ablation.

Another possibility is that the laser ablation of the superconducting film through the relatively thick stabilizer not only removes some amount of superconducting material, as in the case of the control sample, but does substantial additional damage to the remaining superconductor. As the result, the hysteresis loss *per unit of critical current*, which is what Eq. (5) defines, is larger than expected. This consideration underscores the importance of evaluating AC losses relative to the current-carrying capacity of the conductor.

The eddy current loss in this sample is dominated by the copper stabilizer on the back side of the conductor. It is a non-striated strip of copper 20 μm thick, 12 mm wide with the nominal resistivity at 77 K

$$\rho \approx 2.3\times10^{-8}\Omega cm\,.$$

The critical current of this sample in zero field, Fig. 2(a), is 273 A. Thus, the contribution of the eddy current loss in the back side of the surround stabilizer to the value of the slope given by Eq. (6) is

$$\lambda_2^{e-c} \approx 0.9 mm\cdot s\cdot T^{-1}\,. \qquad (8)$$

In the full penetration regime the coupling losses and eddy current losses add up, so that one can expect that the value of λ_2 obtained from Eq. (6) must be smaller than the total slope obtained by fitting the data in Fig. 4. The fact that the calculated contribution of eddy current loss to the value of λ_2, Eq. (8), is greater than the experimental value shown in Fig 4, indicates two possibilities.

One is that the superconducting layer screens the copper strip from magnetic field [23], thus reducing the eddy current loss. However, this effect tends to vanish in the full penetration regime. Another, more plausible, explanation is that the resistivity of copper the stabilizer is made of is greater

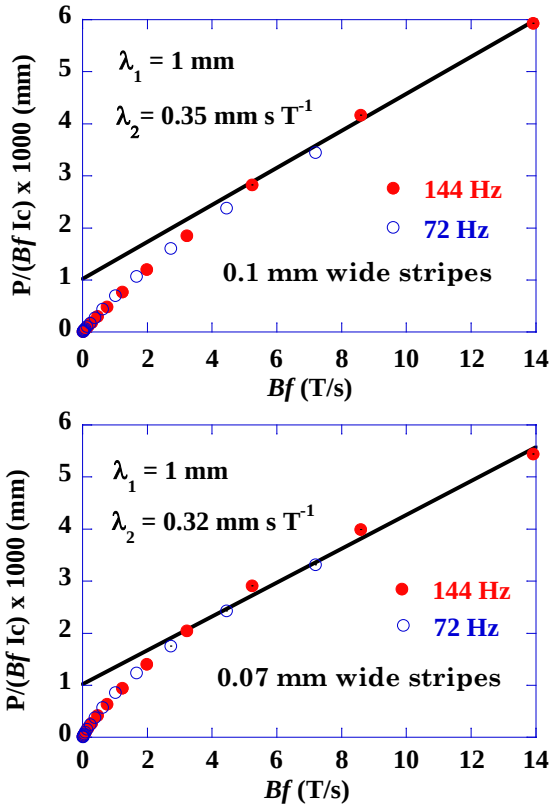

Figure 5. AC power losses in the form of Eq. (5) in another two copper stabilized samples divided into 100 μm and 70 μm wide stripes for two different frequencies 77 and 144 Hz. The grooves segregating the stripes were cut through the 20 μm thick stabilizer and YBCO film. The critical currents are 244 A and 194 A respectively. The straight lines are a linear fit to the data which includes both frequencies.

than the nominal resistivity of copper found in literature and used here. Further study is necessary to clarify this issue.

Figure 5 shows the data for two samples with finer stripes, 100 and 70 μm wide, respectively. The AC loss decreases with increasing number of stripes, but the effect seems to entirely due to removal of superconducting material. Normalized to the critical current, as shown in Fig. 5, the hysteresis loss and the coupling and eddy current losses practically remain the same.

IV. Conclusion

We have attempted a brute force approach to making copper stabilized multifilament coated conductors with the stripe width varying from 200 μm to 40 μm using laser ablation to cut grooves through 20 μm thick stabilizer. The total loss per unit of the critical current is about the same as in striated samples with 1 mm wide stripes. Even if cost is not an issue, striation by laser ablation beyond this limit seems to be ineffective, and other methods of manufacturing more finely striated coated conductors are needed.

Acknowledgment

This work was supported in part by the AFOSR.

REFERENCES

[1] N. Amemiya, S. Kasai, K.Yoda, Z. Jiang, G. A. Levin, P. N. Barnes, and C. E. Oberly, Supercond. Sci. Technol. 17, 1464 (2004)

[2] M.D. Sumption, E.W. Collings, and P.N. Barnes, Supercond Sci. Technol., **18**, 122-134 (2005).

[3] M. Majoros, B. A. Glowacki, A. M. Campbell, G. A. Levin, P. N.

[4] Barnes, and M. Polak, *IEEE Trans. Appl. Supercond.*, vol. 15, p. 2819, 2005.

[5] G. A. Levin, P. N. Barnes, N. Amemiya, S. Kasai, K. Yoda, Z. Jiang, and A. Polyanskii, *J. Appl. Phys.*, 98, 113909, 2005,

[6] P. N. Barnes, M. D. Sumption, and G. L. Rhoads, Cryogenics **45**, 670 (2005).

[7] P. N. Barnes, G. A. Levin, C. Varanasi, and M. D. Sumption, IEEE Trans. Appl. Supercond. 15, 2827 (2005).

[8] V. Selvamanickam et al. IEEE Trans. on Appl. Supercond. 21, 3049 (2011)

[9] S. Terzieva et al. Supercond Sci. Technol., **24**, 145001 (2011).

[10] R. J. Webber, J. Delmas, and B. H. Moeckly, IEEE Trans. on Appl. Supercond. 19, 999 (2009)

[11] H-S. Shin et al. IEEE Trans. on Appl. Supercond. 21 2997 (2011) stabilizer striated

[12] G. A. Levin and P. N. Barnes, IEEE Trans. Appl. Supercond. 15, 2158 (2005).

[13] C. Kwon, J. L. Young, R. G. James, G. A. Levin, T. J. Haugan, and P. N. Barnes, J. Appl. Phys. 101, 0839908 (2007)

[14] Jan Souc, Fedor Gomory and Michal Vojenciak, Supercond. Sci. Technol. 18, 592 (2005)

[15] W. A. Jones et al. Appl. Phys. Lett. **97**, 262503 (2010)

[16] E. H. Brandt and M. Indenbom, Phys. Rev. B **48**, 12893 (1993)

[17] K.-H. Müller, Physica C 281, 1 (1997)

[18] D. N. Nguyen, P. V. P. S. S. Sastry, and J. Schwartz, *J. Appl. Phys.*, 101, 053905 (2007)

[19] W. J. Carr Jr. and C. E. Oberly, IEEE Trans. Appl. Supercond. **9**, 1475 (1999).

[20] G. A. Levin, P. N. Barnes, N. Amemiya, S. Kasai, K.Yoda, and Z. Jiang, Appl. Phys. Lett. 86, 072509 (2005).

[21] G. A. Levin, P. N. Barnes, J. W. Kell, N. Amemiya, Z. Jiang, K. Yoda, and F. Kimura, Appl. Phys. Lett. 89, 012506 (2006)

[22] G. A. Levin, P. N. Barnes, and N. Amemiya, IEEE Trans. Appl. Supercond. **17 (2)**, 3148 (2007)

[23] M. Staines, K. P. Thakur, L. S. Lakshmi, and S. Rupp, IEEE Trans. Appl. Supercond. **19 (3)** 2851 (2009)

Institute of Electrical Engineering
Slovak Academy of Sciences
841 04 Bratislava, Dúbravská cesta 9, Slovak Republic

Performance report

Developing Test Apparatus and Measurements of AC Loss of High Temperature Superconductors

Award No. FA8655-10-1-3079, European Office of Aerospace Research and Development (EOARD)

Program manager: Scott Dudley
Principal investigator: M. Polak
Research team: P. Mozola, J. Souc, D. Erbenova, J. Talapa

Collaboration: P. Barnes,AFOSR
T. Haugan, AFOSR
J. Murphy, AFOSR

Bratislava, August 2011

Table of contents

1. List of Figures
2. List of Tables
3. Summary
4. Introduction
5. Methods, Assumptions and Procedures
6. Results and discussion
7. Conclusions
8. References
9. List of symbols, Abbreviations, Acronyms
10. Appendix

1. List of Figures

Fig.1. The measured values of Volume Flow Rate (VFR) vs. time, liquid nitrogen container Jozef 2 and the calorimeter box.
Fig..2. The corrected values of VFR in standard liter per minute (SLPM) vs heating power.
Fig.3. VFR vs. time measured for the test coil with 1 m of YBCO tape. The turns per minute start at 1200 and were stepwise decreased by 100 RPM. The last value of RPM is 500.
Fig.4. Losses in the test coil vs. frequency
Fig.5. Losses per cycle as a function of frequency, determined using data from Fig. 4.
Fig. 6. The measured data (calibration and coil measurement) modified using a spline function
Fig.7. VFR vs time corrected for no heating VFR
Fig. 8. Calibration curve using the data corrected by the second way.
Fig. 9. Coil losses using the calibration curve in Fig.8.

2. List of Tables

Table 1: Calibration data from Fig.1

3. Summary

We have developed, manufactured and tested a calorimetric apparatus for measurement of AC losses in small test YBCO coils. The external magnetic field was produced by the system of rotating permanent magnets (called SAM machine), developed by the partner laboratory WPAFB. The calorimetric system was successfully tested in the SAM machine. Improvements of the system were proposed after the tests.

A special YBCO pancake coil with slots between the turns was prepared in order to measure magnetic field in the winding space and to compare the results with the calculations. The effect of magnetization currents on the profiles of radial magnetic field in the winding was experimentally determined.
Also the effect of the critical current uniformity across the tape was demonstrated experimentally as well as theoretically. The results will be presented at the 22nd International Conference on Magnet Technology in September 2011 (Marseille, France).

For the next period a common programme focused on AC losses in YBCO filamentary tapes was elaborated. WPAFB (coordinator), Ohio State University and Institute of Electrical Engineering Bratislava are the participants in this programme.

4. Introduction

The first objective of the proposed project was to finish the development and tests of the calorimeter measuring system for AC loss measurements in the AC loss test machine (SAM) built by AFRL/RZPG at Wright-Patterson Air Force Base (WPAFB). The application of high temperature superconductor $YBa_2Cu_3O_{7-x}$ (YBCO) coated conductor wires in electrical power generators for use on airborne platforms can

substantially reduce their weight. Operating frequencies of these power generators are 400 to 500 Hz. At these frequencies the AC losses play an important role and limit the use of the YBCO coated conductors. The experimental and theoretical studies of AC loss problems in the previous periods were done mostly on short samples and small model coils in relatively low magnetic fields (0.1 to 0.2 T). The generation of AC magnetic fields with induction of the order of 1 T and frequencies up to ~500 Hz is a very complicated technical problem. The basic idea of the AC loss test system fulfilling the conditions mentioned above is to rotate a set of permanent magnets fixed to a rotor rotating with high speed which creates magnetic fields with required frequencies. The space between the rotor and the stator will be used for a calorimeter system for AC loss measurements.

The calorimeter system proposed and realized by Institute of Electrical Engineering (IEE) Bratislava consists of the liquid nitrogen container, in which the calorimeter box will be placed. The system was tested together with SAM machine in WPAFB at the end of 2010.

The second objective is to study AC losses in YBCO coils using experimental set-ups existing at IEE Bratislava.

Experimental determination of AC losses in model coils of YBCO in external magnetic fields with frequencies of the order of 100 Hz and amplitudes B_m ~1T at liquid nitrogen temperatures (77 K) represents an important step in the development of superconducting windings for AC use. We studied magnetic field in the winding of a small test YBCO pancake coil wound with 2.33 m of 12 mm wide YBCO tape (manufacturer Super Power Company). Also AC losses were determined theoretically and experimentally. The results will be presented at 22nd International Conference on Magnet Technology to be held in September 2011 in Marseille [1]

The third objective is to study the distribution of magnetization currents in samples of conductors used for winding of test coils.

5. Methods, assumptions and procedures

The basic problems of calorimetric measurements of losses were studied in the frame of previous contracts. The basic problem was the construction of liquid nitrogen containers, which must be made of non-magnetic and non-metallic material. We used the lamination technique, a combination of glass-fiber tissue and epoxy resin suitable for low temperatures. The manufactured container was tested at IEE Bratislava and at WPAFB.
AC losses and magnetic field distribution in an YBCO pancake coil were measured in a special pancake coil. The turns were separated by relatively thick insulation, which was interrupted in several positions. In these slots we inserted thin Hall probe which measured the radial component of the magnetic field. At first, we measured magnetic field in the winding space at relatively low currents at room temperature. At these conditions there are no magnetization currents. Then the measurement was done at 77 K, when magnetization currents considerably affected the field in the winding.

6. Results and discussion

6.1. Evaluation of tests of the calorimetric system performed in WPAFB on October 4 to 8, 2010

Description of performed experiments (T. Haugan)

Three basic experiments were performed:

LN_2 depletion rate test:

The purpose of this experiment was to determine the thermal stability of the calorimeter when installed in the SAM machine. This information is used to determine the length of time data can be taken without interruption for refilling with LN_2.

This test was inconclusive because the depletion rate, due to external, non-sample heating, continues to fall as the machine is conditioned by continuous vacuum pumping and repeated thermal cycling.

HTS Coil in Alternating Magnetic field

This experiment was based on exposing a 1 meter coil of buffered YBCO tape to the SAM magnet operating at varying rotational speeds, providing corresponding frequencies of alternating magnetic fields.

The magnet rotor was spun up to 1200 RPM and the speed was reduced in 100 Rpm steps, resulting in the step-like changes shown in gas flow in the accompanying charts.

The rotor is a four pole Halbach magnet. 1200RPM / 60sec X 4 poles = 80Hz.

Test of Calibration Resistor

This experiment used the Internal Calibration Resistor to generate the gas flow. Power was initially turned on at 150mA and was reduced in 20mA steps.

Due to high background noise and stability problems, the data represented here is somewhat marginal. These two problems improved substantially during the past few days. As operations improve these test will be run again.

6.2. Test results

Calibration

The heating power $P_h = R_h I_h^2$ was stepwise decreased from a maximum to zero (the resistor $R_h = 104\ \Omega$ was supplied by current I_h). The test was started at $I_h = 0.15$ A ; $P_h = 2.34$ W. The volume flow rate (VFR) as a function of time was registered, see Fig.1. The values of "stable" VFR vs. heating power must be corrected, as for $P_h=0$ the value of VFR $\neq 0$. The corrected values of VFR = f(P_h) are given in Table 1.

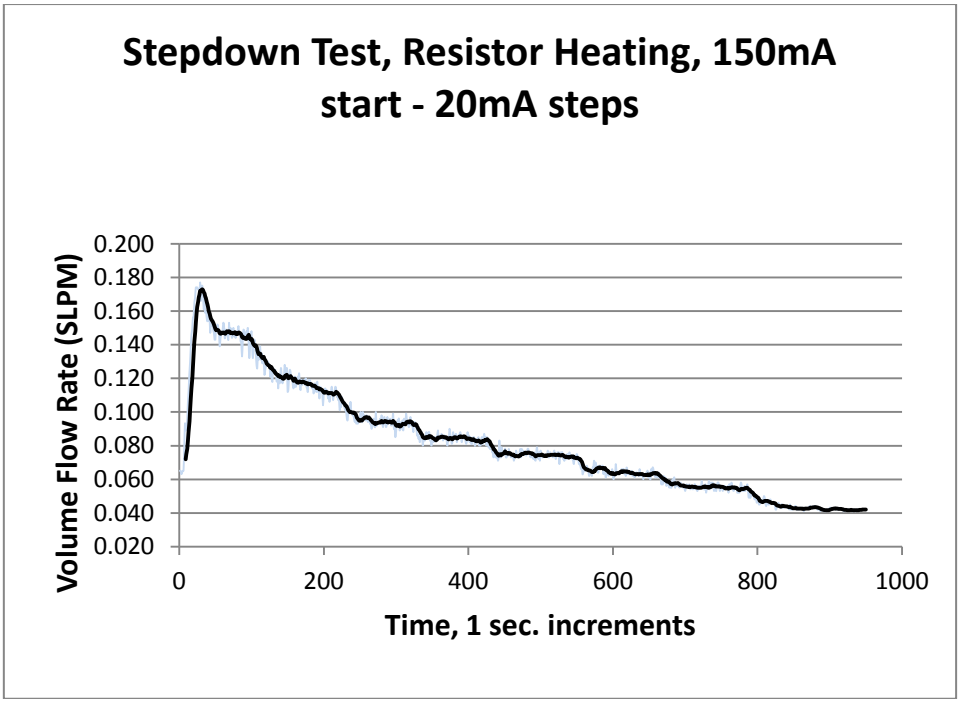

Fig.1. The measured values of Volume Flow Rate (VFR) vs. time

Table 1: Calibration data from Fig.1

I_h(A)	P_h(W)	VFR	VFR corr.
0.1500	2.3400	0.1460	0.1040
0.1300	1.7576	0.1130	0.0710
0.1100	1.2584	0.0930	0.0510
0.0900	0.8424	0.0840	0.0420
0.0700	0.5096	0.0750	0.0330
0.0500	0.2600	0.0640	0.0220
0.0300	0.0936	0.0550	0.0130
0.0000	0.0000	0.0420	0.0000

The calibration curve $VFR_{corrected}$ vs. heating power is shown in Fig.2. According to our previous results this dependence should be linear. As seen in Fig.2, the scatter of the calibration points is quite large. We approximated the measured dependence by a simple linear one with the slope $VFR_{corrected}/P_h = 0.102/2.5 = 0.0408$ SLPM/W.

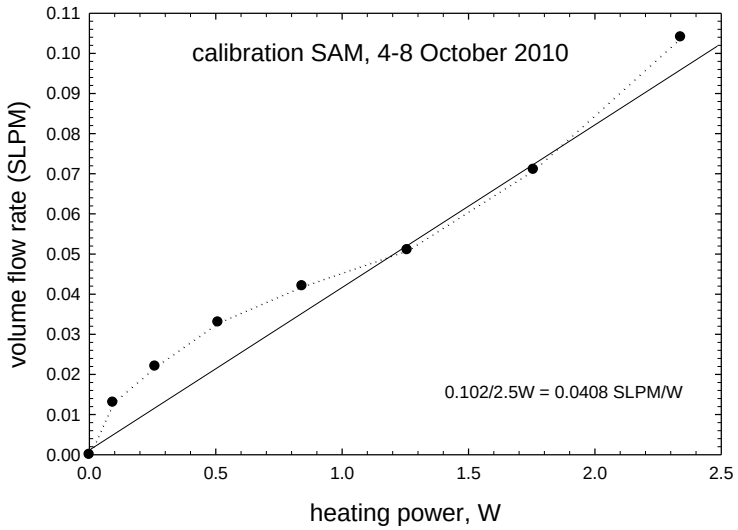

Fig.2. The corrected values of VFR in standard liter per minute (SLPM) vs. heating power. The linear approximation yields the calibration constant
K_{cal} = 0.0408 SLPM/W

The scatter of the measured point is too large and the calibration should be repeated and extended to higher heating power values.

If the flowmeter output is calibrated, we can calculate the calibration points. The heating power of 1W evaporates 0.023liters of liquid nitrogen per hour, which represents 0.023 x 691 = 15.8 liters of nitrogen gas at 300 K per hour. Thus, at 1 W the value of VFR should be 0.263 L/min. This value is about 10 times larger than the value obtained by the calibration. Reason?
Calculation: see Appendix.

6.3. Measurements of coil losses as a function of frequency

VFR vs. time for various frequencies of the magnetic field (amplitude ~ 0.6 T) was registered, as shown in Fig.3.
The measurements were started at frequency 80 Hz, then the frequency was stepwise decreased (steps 100 RPM = 6.67 Hz): 80 Hz, 73.3 Hz, 66.7 Hz, 60 Hz,
53.3 Hz, 46.6 Hz, 40 Hz, 33.3 Hz.

We have a problem how to determine the dependence of the volume flow rate (VFR) on frequency. The problem is caused by a difference of zero heating flow rate at the start of the measurements and that at the end of measurements. As seen in Fig. 3, at the start of the experiment at P_h=0 is VFR= 0.065, while at the end VFR = 0.03. Shortly before the end the SAM machine was switched off and on, which could affect the FR (both switching off and on generate losses and affect FR).
Thus, we can evaluate the measurements by two ways:
a. We supposed that the zero heating flow rate is correct at the begin of the measurements only (0.065 SLPM)
b. We supposed that the zero heating flow rate at the begin as well as at the end are correct and VFR changes linearly with time between the begin and the end.

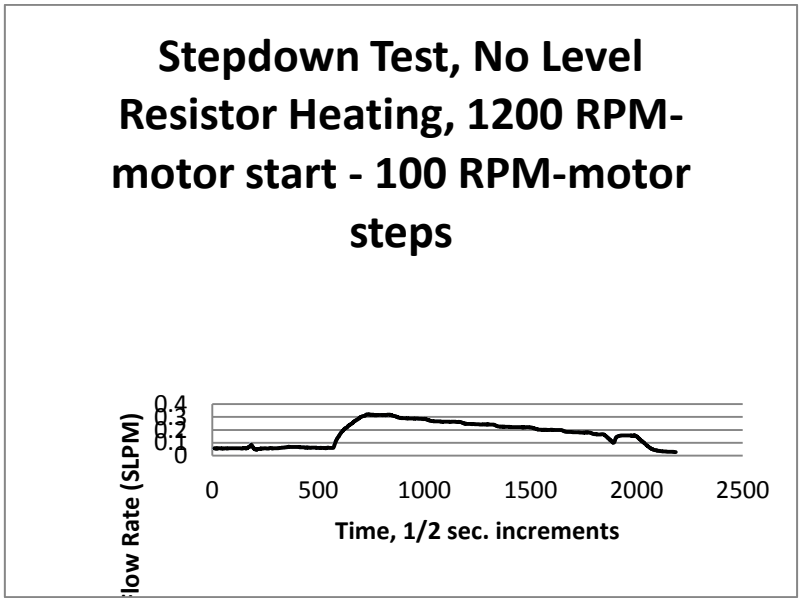

Fig.3. VFR vs. time measured for the test coil with 1 m of YBCO tape. The turns per minute start at 1200 and were stepwise decreased by 100 RPM. The last value of RPM is 500.

At first, we supposed that the value of VFR at the start of the measurements is correct. We estimated VFR at each frequency (f=RPM x 4/60) and corrected VFR values ($VFR_{coorected}$= VFR – 0.065). Then, using the calibration constant K_{cal} = 0.0408 SLPM/W we calculate the losses corresponding to the frequency. By this way we obtained the dependence of loss power on frequency, as shown in Fig. 4.

In Fig.5 we show the values of loss per cycle determined using data in Fig. 4. We see that the losses per cycle depend on f very litle, as expected. The main loss component is the frequency independent hysteresis loss.

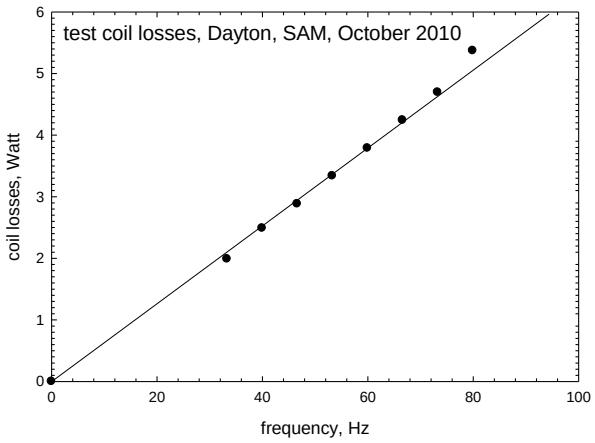

Fig.4. Coil losses vs. frequency

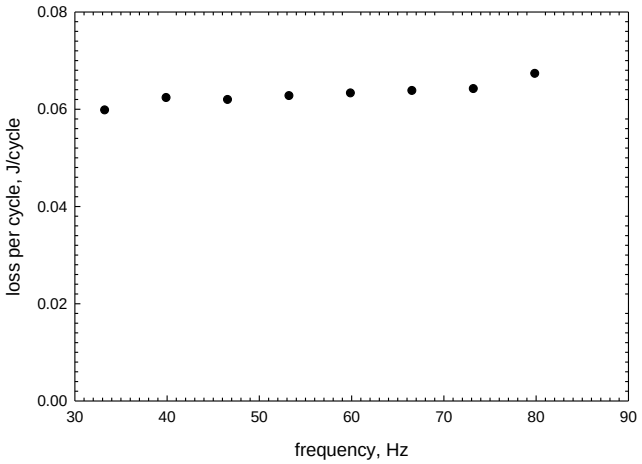

Fig.5. Losses per cycle as a function of frequency, determined using data from Fig. 4.

Evaluation using a supposition that VFR changes linearly with time between the begin and the end.

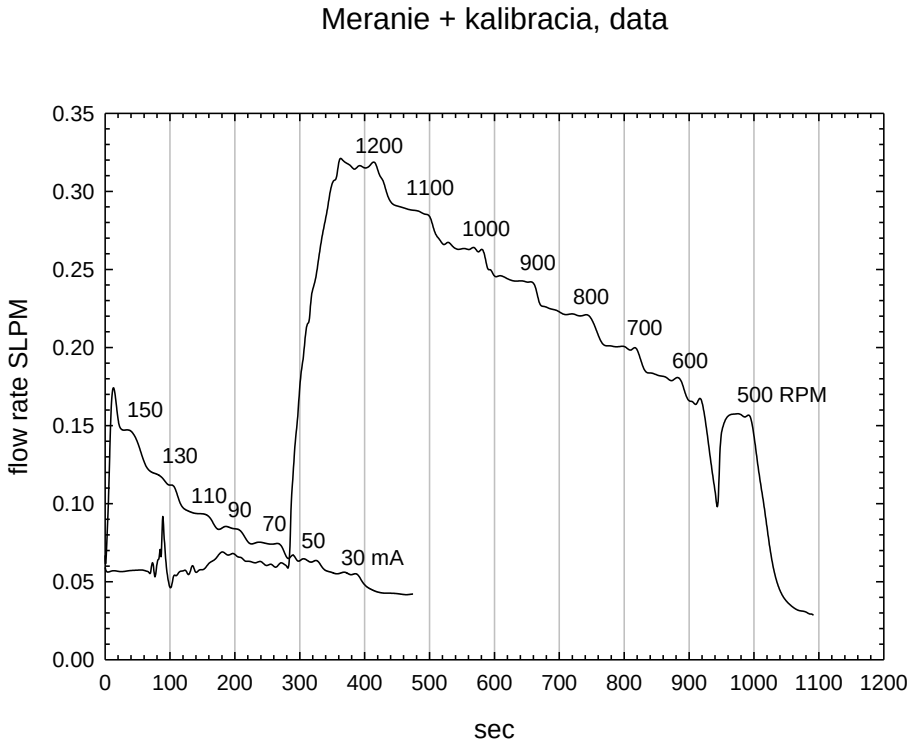

Fig. 6. The measured data (calibration and coil measurement) modified using a spline function

In Fig.7 we show the data (both calibration and coil measurements) corrected using a linear change of no heating VFR

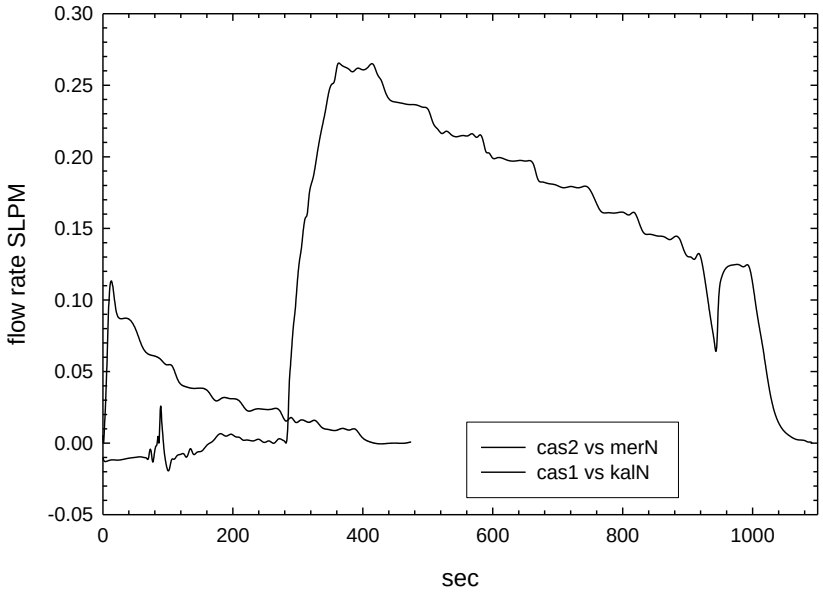

Fig.7. VFR vs time corrected for no heating VFR
The calibration curve obtained from Fig. 7 is shown in Fig.8

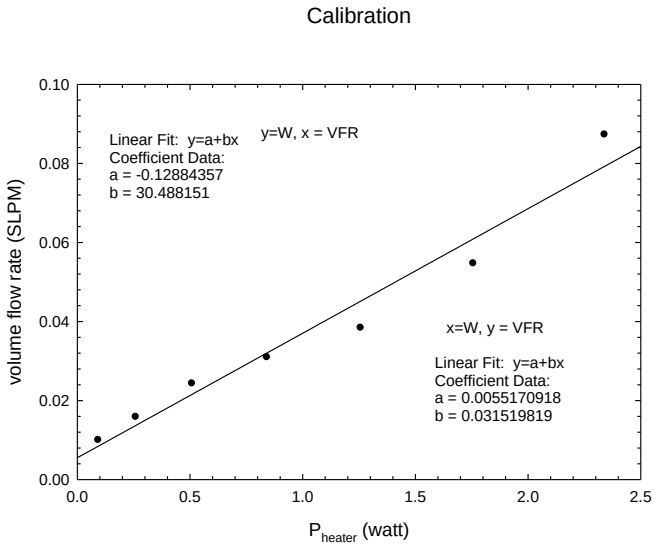

Fig. 8. Calibration curve using the data corrected by the second way. More data at higher heating power values would be necessary.

The coil losses evaluated using calibration curve shown in Fig.8 are given in Fig.9. We see higher losses than those obtained using the first evaluation method.

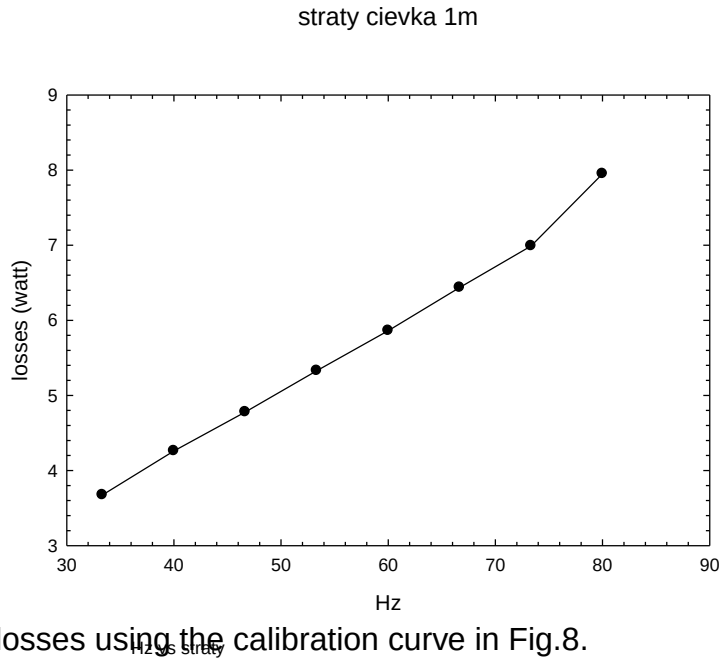

Fig. 9. Coil losses using the calibration curve in Fig.8.

In Fig.10 we show the coil losses per cycle obtained from Fig. 9. They decrease with increasing frequency which indicated some errors.

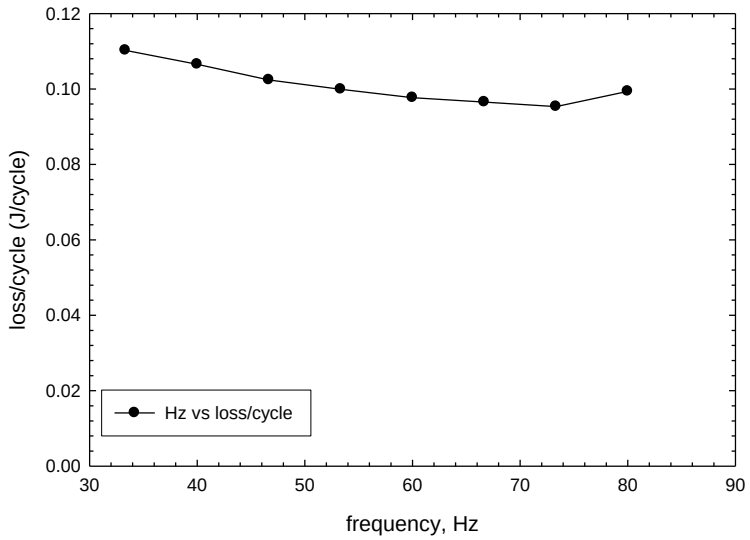

Fig.10. Coil losses as a function of frequency.

The calibration should be done also at higher heating power values.
As we have observed earlier, additional heating should be used to increase the precision of the experiment. The additional heating can be generated by the same resistor as that used for calibration (we start at $I_h>0$).
Magnetic field amplitude and time profile should be determined using pick up coils or Hall probes.
Parameters of the test coil should be given.

6.4. Magnetic field in the winding space of an YBCO test coil, calculation and measurements of AC losses.

The radial component of the magnetic field in the winding space of a pancake coil controls AC losses in the coil. The calculations must take into account the existence of magnetization currents.
For the calculations we need to know all relevant parameters of the tape we use for the winding.
We studied theoretically and experimentally the radial field component and AC losses in an YBCO test coil wound with 2.32 m 12 mm wide YBCO tape Super Power.
The results are summarized in a paper which will be presented at 22nd International Conference on Magnet Technology (September 2011, France).
The full paper text is in the Appendix.

7. Conclusions

Calorimetric system.
The tests of the calorimeter together with SAM machine showed that AC losses of the test coil at 30 Hz are about 3.5 W. Calorimeter sensitivity limit is of about 10 mW. Problems with the tightness must be solved. One of possible reason is the quick cooling.
Calculation and measurements of the radial magnetic field component in a test YBCO coil.
AC losses in a test YBCO coil wound with 12 mm wide tape were determined theoretically and experimentally. The total tape length used in the coil is 2.32 m. The loss per cycle is practically frequency independent and is about 0.01 J at I=100 A and frequencies from 22 Hz to frequencies of the order of 100 Hz.
We have found that the critical current per unit width of the tape we used is the highest at the tape edges. In the tape center it is lower by about 30%. The calculated AC losses are higher in the case of a uniform distribution of the critical current density.
The full text of the paper for MT 22 is in the Appendix.

8. References

[1] M. Polák, E. Pardo, P. Mozola, J. Šouc, Magnetic field in the winding of an YBCO pancake coil: experiments and calculations, to be presented at MT 22, September 2011, Marseille, France

11.List of symbols, Abbreviations, Acronyms

WPAFB – Wright Patterson Air Force Base
IEE – Institute of Electrical Engineering
VFR – Volume Flow Rate

YBCO $YBa_2Cu_3O_x$
HTS – High Temperature Superconductors
AC – Alternating Current
Hz – Hertz (frequency)
LN_2 – liquid nitrogen
SAM – spin around magnet

APPENDIX:
1IO2

Magnetic field in the winding of an YBCO pancake coil: experiments and calculations

M. Polák, E. Pardo, P. Mozola, J. Šouc

***Abstract*—Many promising applications of ReBCO coated conductors contain pancake coils, like high-field magnets, transformers, motors and generators. However, the AC loss in these coils is too high. In order to reduce the AC loss, it is necessary to understand the loss mechanisms. We measured and computed the radial magnetic field component in a pancake coil with a net transport current, as this component of the magnetic field plays a crucial role in the AC loss. For this purpose, we prepared a small pancake coil wound with 12 mm wide YBCO tape with non-magnetic substrate and measured the radial component of the magnetic field in the space between turns at both 77 K and room temperature. We measured at six radial positions inside the coil winding during the first AC cycle and the following ones. Besides, we numerically calculated the magnetic field in all the pancake coil, taking into account the hysteretic nature of the supercurrents. The agreement of the calculated and measured profiles of radial component proves that the calculation method is correct. The radial component at room temperature, when the YBCO is not superconducting, is not hysteretic. In conclusion, the comparison of the experimental values of the radial field component at room temperature and 77 K provide information on the hysteretic currents in the superconductor. Moreover, our simulation method for the calculations is useful to predict the AC loss and the hysteretic effects of pancake coils.**

***Index Terms*—Superconducting coils, High temperature superconductors, Loss measurement, Magnetic field measurement.**

I. INTRODUCTION

HIGH temperature superconductors (HTS) are attractive for various AC applications. Twenty six YBCO single pancake coils centered on a stainless steel former will be used in a commercially viable HTS transformer operating at high voltage (138 kV) [1]. Experimentally determined AC losses in the pancakes close to the coil ends were considerably higher than those in the central part. Another example is a 20 MVA class superconducting transformer developed in Japan [2]. In Europe there are also several projects for AC applications of YBCO in superconducting electrical machines [3].

Manuscript received 12. September 2011. This work was supported in part by the Air Force Office of Scientific Research, Air Force Material Command, USAF, under grant number FA8655-10-1-3079, by Euratom FU-CT-2007-00051 and by Structural Funds of the European Union, contract no. 26240220028.

M. Polák (Milan.Polak@savba.sk, phone 00421 2 5922 2347), E. Pardo (Enric.Pardo@savba.sk), P. Mozola (Pavol.Mozola@savba.sk) and J. Šouc (Jan.Souc@savba.sk) are with the Institute of Electrical Engineering, Dubravska 9, 84104 Bratislava, Slovakia

AC losses cause heating of the superconductor. At operating temperatures 77 K (liquid nitrogen) the heat produced by loss power of 1 W requires about 20 W of the refrigeration power [4]. Serious investigations need to be made in the area of AC losses to make superconducting devices competitive with conventional systems.

YBCO coils carrying AC currents with industrial frequencies can be wound with relatively wide YBCO tapes (4 to 12 mm) or the tapes can be divided into several stripes to reduce the total AC losses. However, the results presented in [5] indicate that I-V curves of coils using striated tapes show quite flat I-V curves, hence the power is also dissipated at current far below the critical current of the tape. Ishiguri and Funamoto proposed a graded coil with improved critical current [6].

The calculation and measurements of losses in single pancake coil is also of interest because usually the pancakes are experimentally tested individually. Some numerical models have been developed for tapes and coils [7], [8], [9], [10].

For all calculations of magnetic fields and AC losses in pancake coils it is very important to know all relevant properties of YBCO tape used. First of all we need to know the voltage - current curves in various external magnetic fields applied perpendicular to the tape plane, from which the critical current I_c is determined. It is usually supposed that for currents flowing parallel to the tape axis the critical current per unit width, $I_{c1}=I_c/w$ (w is the tape width), is uniform and independent on the lateral coordinate [11]. The dependence of I_{c1} on the angle α between the magnetic field vector and the tape plane (anisotropy of I_{c1}) must be also known, unfortunately, this parameter changes from tape to tape. Moreover, it is also supposed that the anisotropy is also uniform in each point of the tape.

In this work we studied current-voltage curves, $I_c(B)$ and anisotropy of commercially available 12 mm wide YBCO tape manufactured by Super Power. Also the uniformity of longitudinal I_{c1} as a function of the lateral position was carefully studied.

Then, an experimental YBCO pancake coil with a special winding structure allowing the measurement of the radial magnetic field component inside the winding was prepared. Using the tape parameters determined experimentally we numerically calculated the magnetic field in all the pancake coil, taking into account the hysteretic nature of the supercurrents. The calculated radial component of the magnetic field are compared with the measured ones. We also

calculated and measured coil losses in the frequency range from 22 Hz to 135 Hz.

II. EXPERIMENTAL

A. Tapecharacteristics

The pancake coil was wound with 12 mm wide YBCO tape Super Power, type Super Power SCS 12050 with the cross section of 12 mm x 0.09 mm. Hastelloy substrate was 0.05 mm thick, the YBCO layer (~1 um thick) was covered by 2 μm thick Ag layer and stabilized by 0.02 mm thick copper layer. The measured dependence of the tape critical current on magnetic field B at 77 K, I_c(1μV/cm) is shown in Fig.1. The critical current non-uniformity in the longitudinal direction was smaller than 5% on the length scale of the order of 1 m (given by the manufacturer).

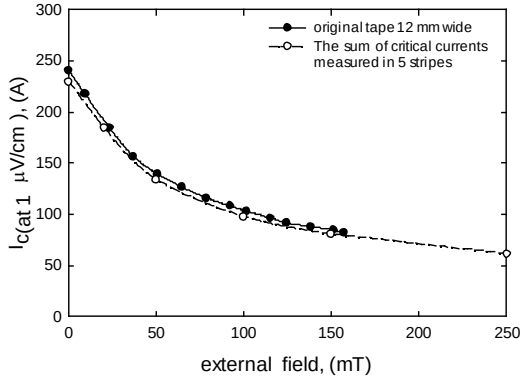

Fig. 1. Critical current I_c vs. external magnetic field applied perpendicular to the tape plane, tape width 12 mm, T=77K (full symbols). Also the sum of critical currents measured in 5 stripes in which the tape was subdivided by longitudinal cuts is shown (open symbols). The cuts reduced the effective sum of the tape width by ~5%, the corresponding corrections are done.

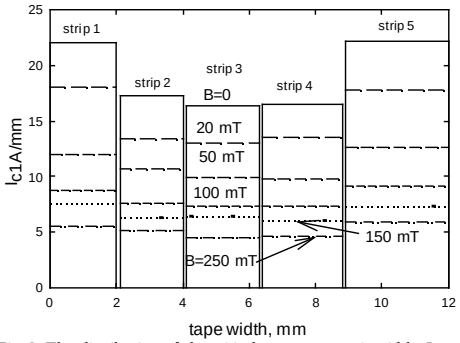

Fig. 2. The distribution of the critical current per unit width, I_{c1}, across the tape, measured at various magnetic fields.

We also tested the uniformity of the longitudinal critical current distribution across the tape width. For this purpose we divided about 15 mm long tape piece into 5 stripes using a fine wire saw. The width of the stripes varied between 2 and 3 mm. Then, we measured the critical currents I_c of the stripes at various external fields and determined the critical current per unit width in each stripe: $I_{c1} = I_c/w$ (w is the width of the stripe). The results are shown in Fig. 2. The values of I_{c1} are higher by about 30 % at the tape edges than in the tape center.

We also measured the dependence of I_{c1} in all 5 stripes on angle α between the stripe plane and the direction of the external magnetic field (for the perpendicular field $\alpha=0^0$). As an example, in Fig.3 we show $I_{c1} = f(\alpha)$ measured for a strip cut from the tape edge. While at 20 mT $I_{c1}(0^0)/I_{c1}(90^0)$ ~1.16, this ratio at 250 mT is much higher (~ 1.8). We note that the anisotropic behavior of stripes cut from different tape area was also different.

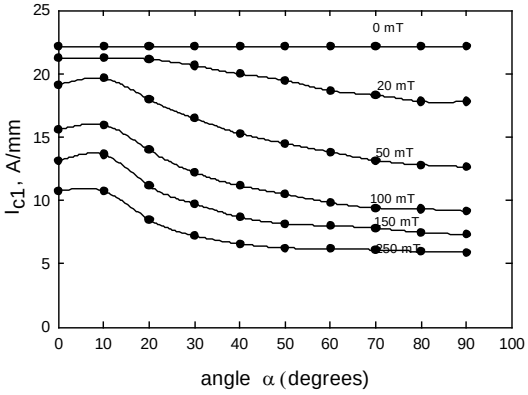

Fig. 3. The dependence of the critical current per unit width on angle α measured for stripe 5.

B. The parameters of the coil

The main parameters of the coil are shown in Table I. In (r, z) coordinate system the coil axis is z, the radial coordinate is r. The tape resistance of 12 mm wide tape at room temperature was 3.00 x 10^{-3} Ω/m. The resistance of the coil at room temperature was 7 x 10^{-2}Ω, the tape length in the coil was 2.32 m.

TABLE I THE MAIN PARAMETERS OF THE COIL

Inner diameter	30 mm	Length of the mean turn	0.1287 m
Outer diameter	52 mm	Effective thickness of 1 tum	0.61 mm
Width	12 mm	Total tape length	2.32 m
Number of turns	19	Coil inductance at 300 K, f=100 Hz	12.72 mH

To be able to measure the magnetic field in the winding volume, we used a thick inter-turn insulation (about 0.4 mm). We prepared 6 slots in the coil, in which we measured the radial magnetic field (see Fig.4). A thin glass-fiber support plate with a small Hall probe was used for measurement of the radial field component (see also Fig.4).

The positions of the slots: 1st. slot: between turns 2 and 3, 2nd slot: between turns 6 and 7, 3rd slot: between turns 11 and 12, 4th slot: between turns 12 and 13, 5th slot: between turns 13 ad 14 and 6th slot: between turns 18 and 19.

The sensitivity of the Hall probe at the control current of 15 mA is 144.3 mV/T at room temperature and 147 mV/T at 77 K.

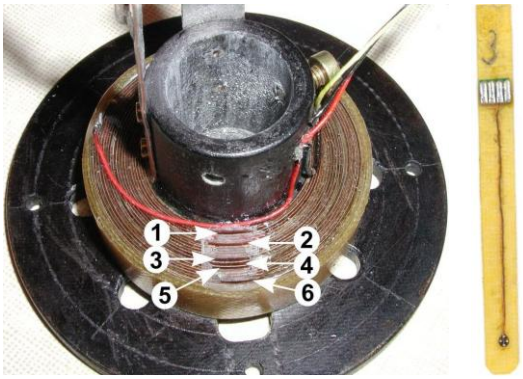

Fig. 4. The coil with 6 slots. At the right side we show Hall probe holder.

III. RESULTS

A. Simulations

We calculated the current distribution and the AC loss in the coil by means of the Minimum Magnetic Energy Variation (MMEV) method, as we did in [10, 11]. This method takes into account the hysteresis of the current distribution, the actual aspect ratio of the superconducting layer, non-uniform critical current density, J_c, a J_c depending on the magnetic field and the orientation angle α, $J_c(B, \alpha)$, and any combination of DC or AC applied magnetic field and transport current in each superconducting tape. The only assumption of the model is the sharp E(J) relation of the critical-state model, where E is the electric field. In our experiments we use the value of the critical current per unit width, $I_{c1} = I_c/w$, where w is the tape width. The value J_c used in the calculations is defined as $J_c=I_c/(w.d)$, where w and d are the width and thickness of YBCO layer. The relation between J_c and I_{c1} is $J_c=I_{c1}/d$. The only input of the program are the dimensions of the coil and the coated conductor and the dependence of the critical current density on the position, the magnetic field and its orientation defined by angle α

For the position dependence of J_c, we use the measurements of critical currents in the stripes independently (see Fig.2). For our coil, we use the measured dependence for 50 mT perpendicular to the tape surface for two reasons: first, in order to minimize the effect of the self-field in the measurements and, second, because this field is of the same order of magnitude as the radial magnetic field in the measurements for the coil. We extract $J_c(B,\alpha)$ from measurements of the critical current in an applied magnetic field. For this, we adjust a realistic formula for $J_c(B,\alpha)$ in such a way that the difference between the calculated in-field critical current and the measured one is minimum for a set of measured B and α, as we did in [12]. For the simulation in this article, we take the measured data for a 4 mm wide tape with similar properties as the 12 mm wide tape of the coil. The obtained J_c is

$$J_c(B,\alpha)=\left\{\left[\frac{J_{0ab}}{\left(1+\frac{Bf(\alpha)}{B_{0ab}}\right)^{n_{ab}}}\right]^m+\left[\frac{J_{0c}}{\left(1+\frac{B}{B_{0c}}\right)^{n_c}}\right]^m\right\}^{\frac{1}{m}}$$

with $f(\alpha)=\sqrt{v^2\cos(\alpha-\delta)^2+u^2\sin(\alpha-\delta)^2}$

where: v=1 for $\cos(\alpha-\delta)<0$ and $v=v_0$ otherwise. The parameters in the equations above are m=8, $J_{0ab}=1.53\cdot10^{10}$ A/m^2, $J_{0c}=1.28\cdot10^{10}$ A/m^2, B_{0ab}=414 mT, B_{0c}=90 mT, n_{ab}=0.934, n_c=0.8, v_0=1.2, δ=-2.5° and u=5.5. Comparing with in-field critical-current measurements of the 12 mm tape of the coil, this J_c over-estimates the one for the 12 mm tape by around 10%.

B. Measured and calculated radial field components at room temperature

We measured and calculated the radial field component B_r in all 6 slots at room temperature and coil current of 5 A. The results are shown in Fig.5a and Fig. 5b.

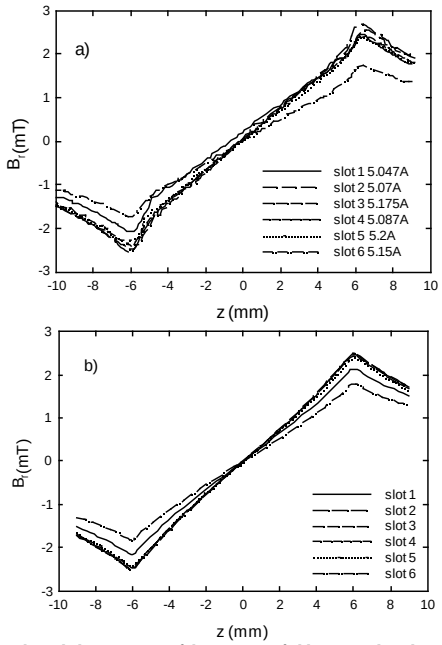

Fig. 5. The radial component of the magnetic field measured in slots 1 to 6 at room temperature and current I=5A: a). The calculated profiles are shown in Fig. b).

The measured and calculated profiles agree very well.

C. Measurements and calculations of the radial field component at 77

We do not show the calculations $B_r=f(z)$ for the virgin cycle, as they are not relevant for AC losses. At first, we calculated the radial magnetic field component $B_r=f(z)$ for coil current decreasing from 80.6 A down to 0 and then increasing to –80.6 A. We assume the real non-uniform current distribution across the tape corresponding to Fig.2. The results obtained for slot 4 are shown in Fig. 6. Very similar curves were calculated for uniform critical current distribution.

The results of measurement of profiles $B_r=f(z)$ for coil current changing stepwise from 80.6 A to –80.6 A (the same steps as in Fig. 6) are shown in Fig. 7. Also curves $B_r=f(z)$ measured at lower currents and linearly extrapolated to 40 A and 80.6 A are shown in the Figure.

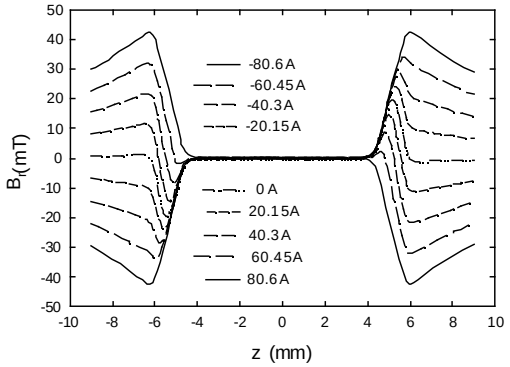

Fig. 6. The calculated values B_r vs. z in slot 4. We supposed the real non-uniform distribution of I_{c1}. The curves are calculated for coil current, changing as follows (left part, from the bottom): 80.6 A, 60.45 A, 40.3 A, 20.15 A , 0, -20.15 A, -40.3 A, -60.45 A, -80.6 A.

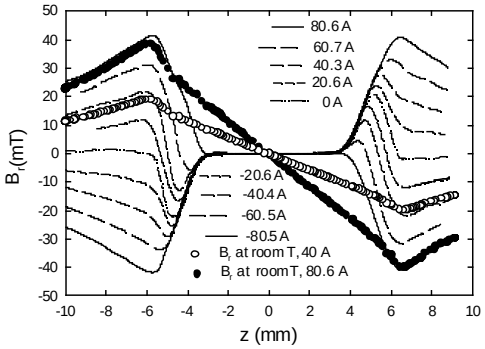

Fig. 7. The measured radial field components measured at current changing from 80.6 A to –80.5 A at 77 K. Also B_r measured at room temperature and current 5 A and extrapolated to 40 A and 80. 6 A are plotted.

In Fig. 7 we clearly see that the magnetization currents affect the radial field component considerably and profiles $B_r=f(z)$ at 300 K and those at 77 K are very different.

D. AC losses

AC losses were measured by a standard lock-in technique. The dependence of losses on the coil current measured at frequencies from 22.5 Hz up to 135 Hz is shown in Fig. 8.

In the figure we also show the losses calculated with the assumption of the uniform critical current density in the tape and the real non-uniform distribution. We clearly see a difference, in particular at lower fields, is of about 25 %.

IV. CONCLUSIONS

We have experimentally determined that the distribution of the sheet critical current density across the tape width in commercially available, 12 mm wide YBCO tape, which we used to prepare a pancake coil, is non-uniform. In the central

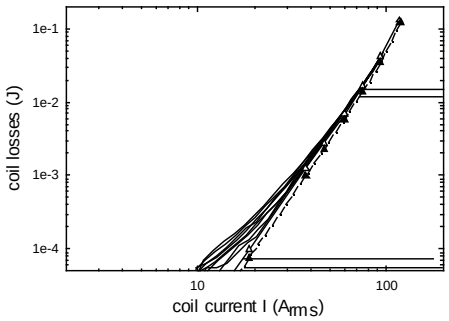

Fig. 8. Coil losses measured at frequencies from 22.5 to 135 Hz. Calculated losses: π - non-uniform current density, ρ -uniform current density

part of the tape the sheet critical current density is by about 30% lower than that at the tape edges. The calculations of coil losses using the real sheet critical current distribution and those using a uniform current distribution showed that the calculations with uniform critical current density indicate larger losses (by about 25 %). Frequency dependence of loss per cycle is small.

Large differences between the magnetic field distribution in the winding of a pancake coil measured at 300 K (no magnetization currents) and 77 K (full magnetization currents) were observed.

ACKNOWLEDGMENT

The authors thank to J. Talapa and D. Erbenova for the technical support.

REFERENCES

[1] C. M. Rey, R. C. Duckworth, S. W. Schwenterly, E Pleva, "Electrical AC loss measurements on a 2G YBCO high voltage coil," IEEE Trans. on Appl. Superconductivity , vol. 21, pp. 2424-2427, June 2011.

[2] N. Fujiwara, H. Hayashi, S. Nagaya, Y. Shiohara, Development of YBCO power devices in Japan, Physica C, vol. 470, pp. 980-985, 2010.

[3] P. Tixador, Development of superconducting power devices in Europe, Physica C, vol. 470, pp. 971-979, 2010.

[4] M. D. Ainslie, V. M. Rodriguez-Zermeno, Z. Hong, W. Yuan,T. J. Flack, T.A.Cooms, An improved FEM model for computing transport AC loss in coils made of RABiTS YBCO coated conductors for electric machines, Supercond. Sci. Technol. vol. 24, 045005, 2011.

[5] H. Okamoto, H. Hayashi, A. Tomioka, M. Konno, M. Owa, A. Kawagoe, F. Sumiyoshi, M. Iwakuma, K. Suzuki, T. Izumi, Y. Yamada and Y. Shiohara, AC loss properties in YBCO model coils for loss reduction, Physica C, vol. 468, pp.1731-1733, 2008.

[6] S. Ishiguri, T. Funamoto, Performance improvement of a high – temperature superconducting coil by separating and grading the coil edge, Physica C, vol. 471, pp.333-337, 2011.

[7] N. Sekine, O. Tsukamoto, A. Utsunomiya, D. Miyagi, Physica C 426-431 (2005) 1284.

[8] N. Amemyia, N. Enomoto, Z. Jiang, S. Kasai, T. Saitoh, Y. Shiohara, AC loss characteristics of coated conductort and the perspective for its AC loss reduction, Physica C, vol. 426-431, pp.1267-1275, 2005.

[9] E. Pardo, Modeling of coated conductor pancake coils with a large number of turns, Supercond. Sci Technol. 21 art. no. 065014, 2008.

[10] Šouc, J., Pardo, E., Vojenčiak, M., and Gömöry, F.: Theoretical and experimental study of AC loss in high temperature superconductor single pancake coils, Supercond. Sci Technol. 22, 015006, (2009).

[11] J. Pitel, P. Kovac, Influence of external magnetic fields on critical currents of solenoids wound with anisotropic HTS tapes-theotretical approach, Supercond. Sci. Technol. 10 847, 1997.

Institute of Electrical Engineering
Slovak Academy of Sciences,
841 04 Bratislava, Slovakia

Calorimeter for AC loss measurements

Dagmar Erbenová, **Pavol Mozola,**
Milan Polák, Jozef Talapa

October 2010

The objectives of the collaboration WPAFB/IEE Bratislava

To develop and test a calorimeter for AC loss measurements in the SAM machine

Measure AC loss in IEE Bratislava and compare the results with those obtained in SAM machine

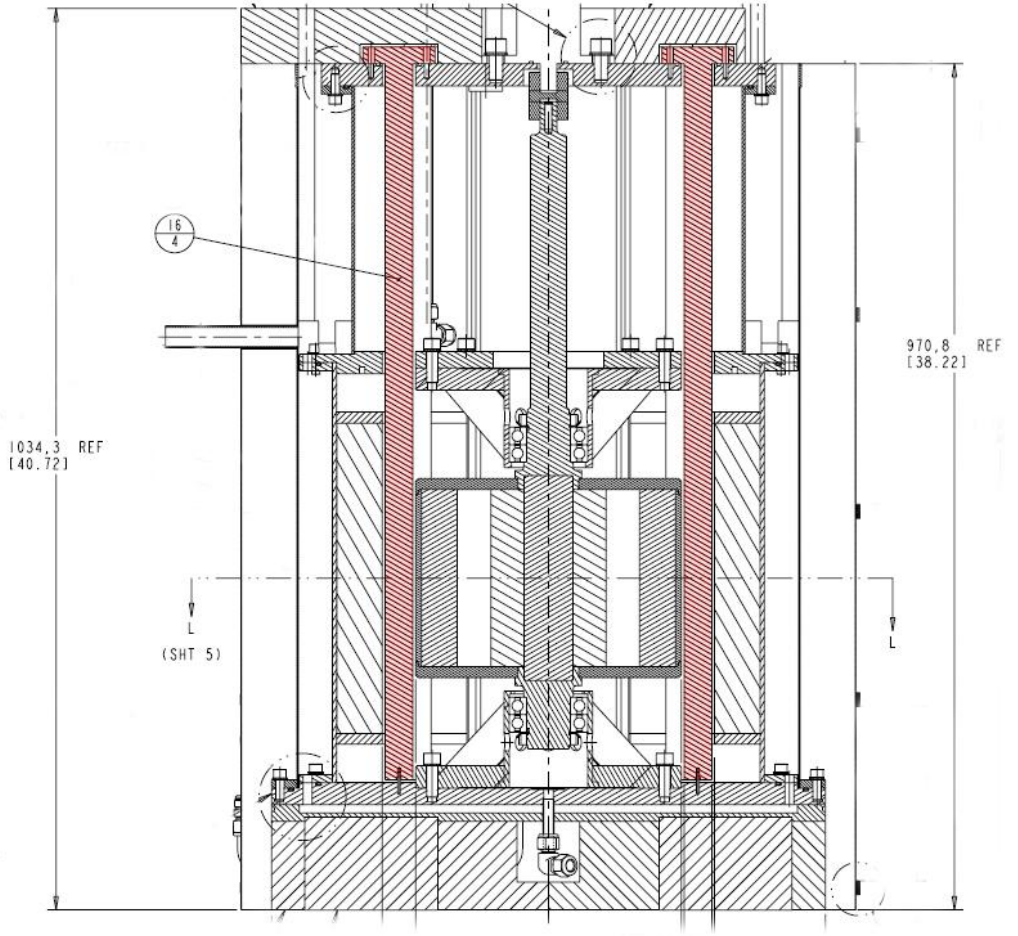

Requirements for the LN_2 container

- it must be vacuum tight
- it must resist to cooling/heating cycles
- the deformation of the walls must not exceed the required values
- it must have a space for inserting the calorimeter box

Conceptual design of the calorimeter

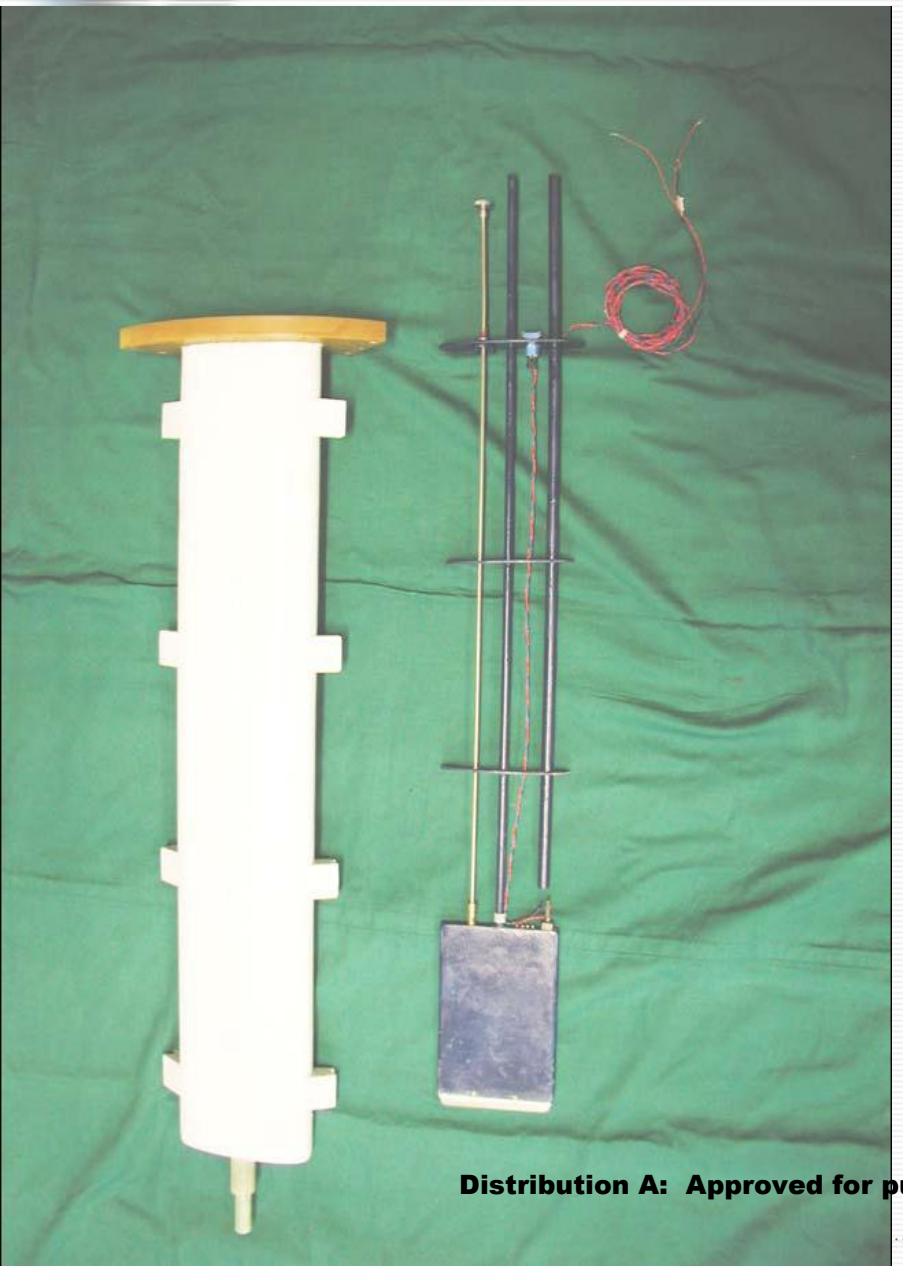

The calorimeter has 2 parts

1. Liquid nitrogen container
2. Calorimeter box with the measured coil

The liquid nitrogen container is made by lamination technique

15 layers of glass fiber tissues were wound on a former and impregnated by epoxy resin

The calorimeter box is also manufactured by a lamination technique.

Requirements for the calorimeter box

- Enough space for test coils 4 to 5 mm thick and diameter up to 100 mm
- Low evaporation rate determining the sensitivity of loss measurements
- It should be equipped with liquid level meter and heating resistor for the calibration

Drawings of the device, photographs

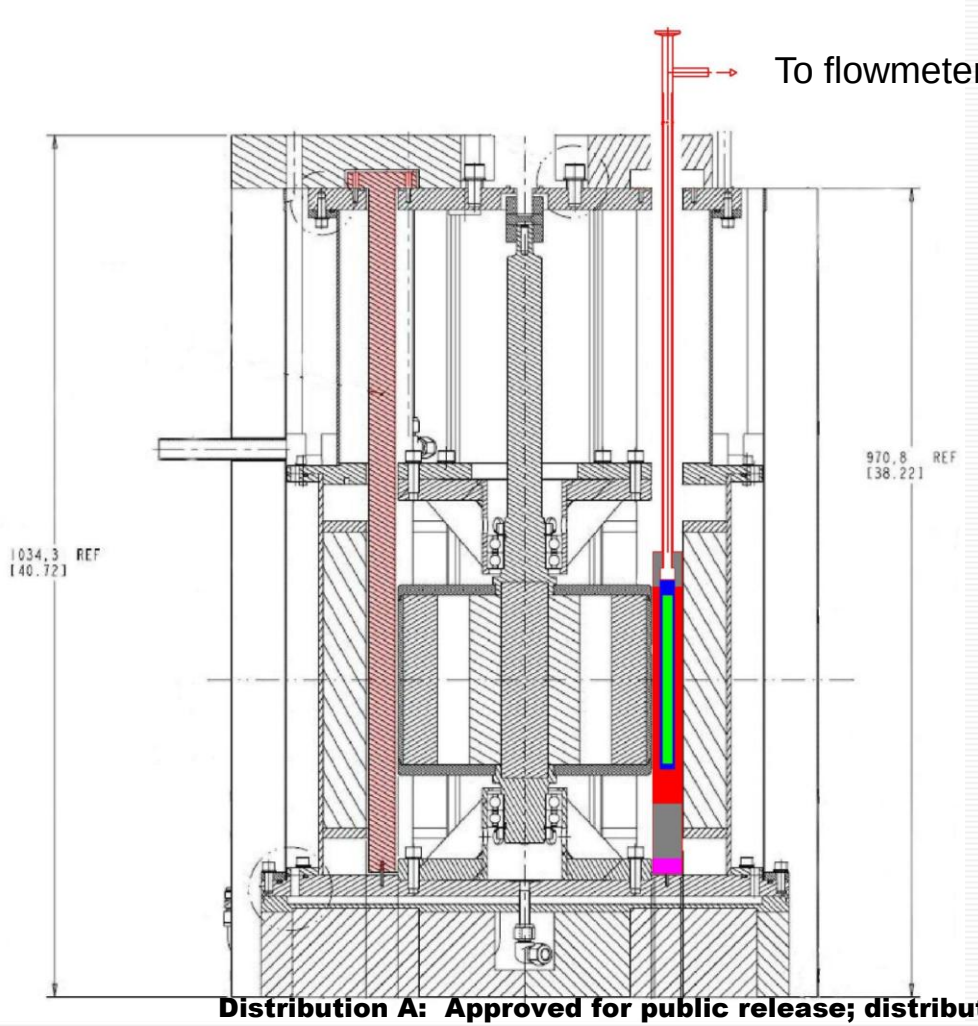

Drawings of the device, photographs

Final version of the calorimeter box

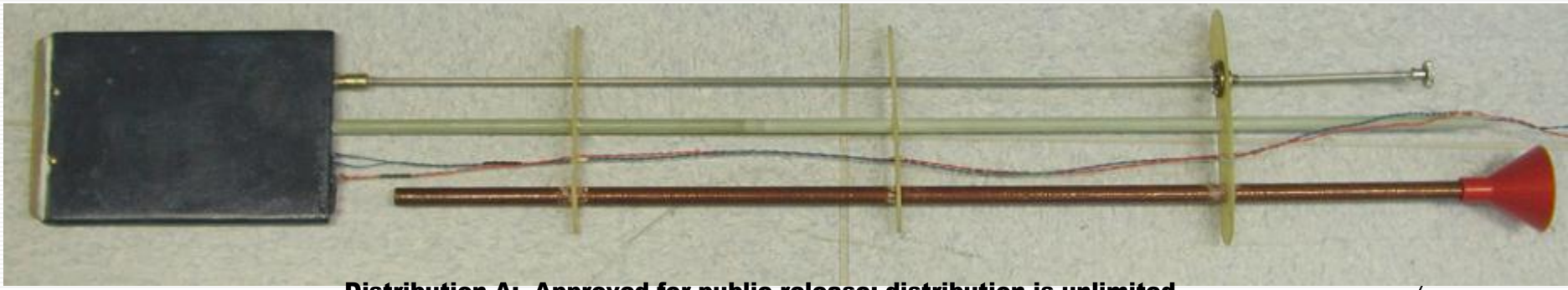

Drawings of the device, photographs

Alternative version of the calorimeter box

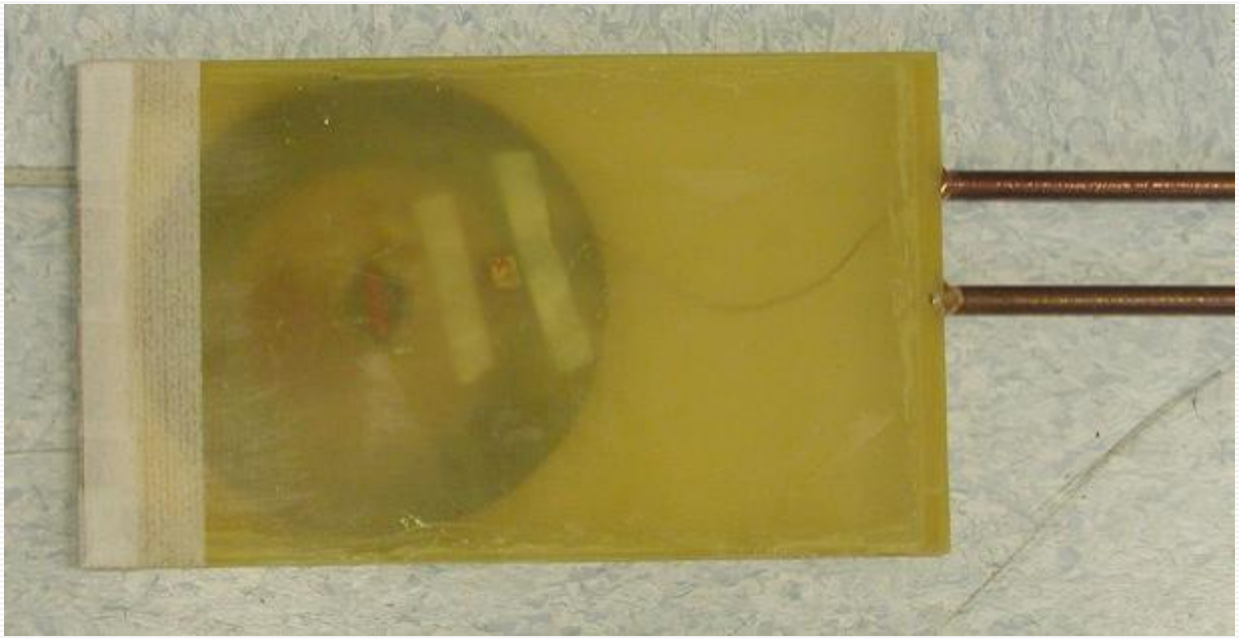

Drawings of the device, photographs

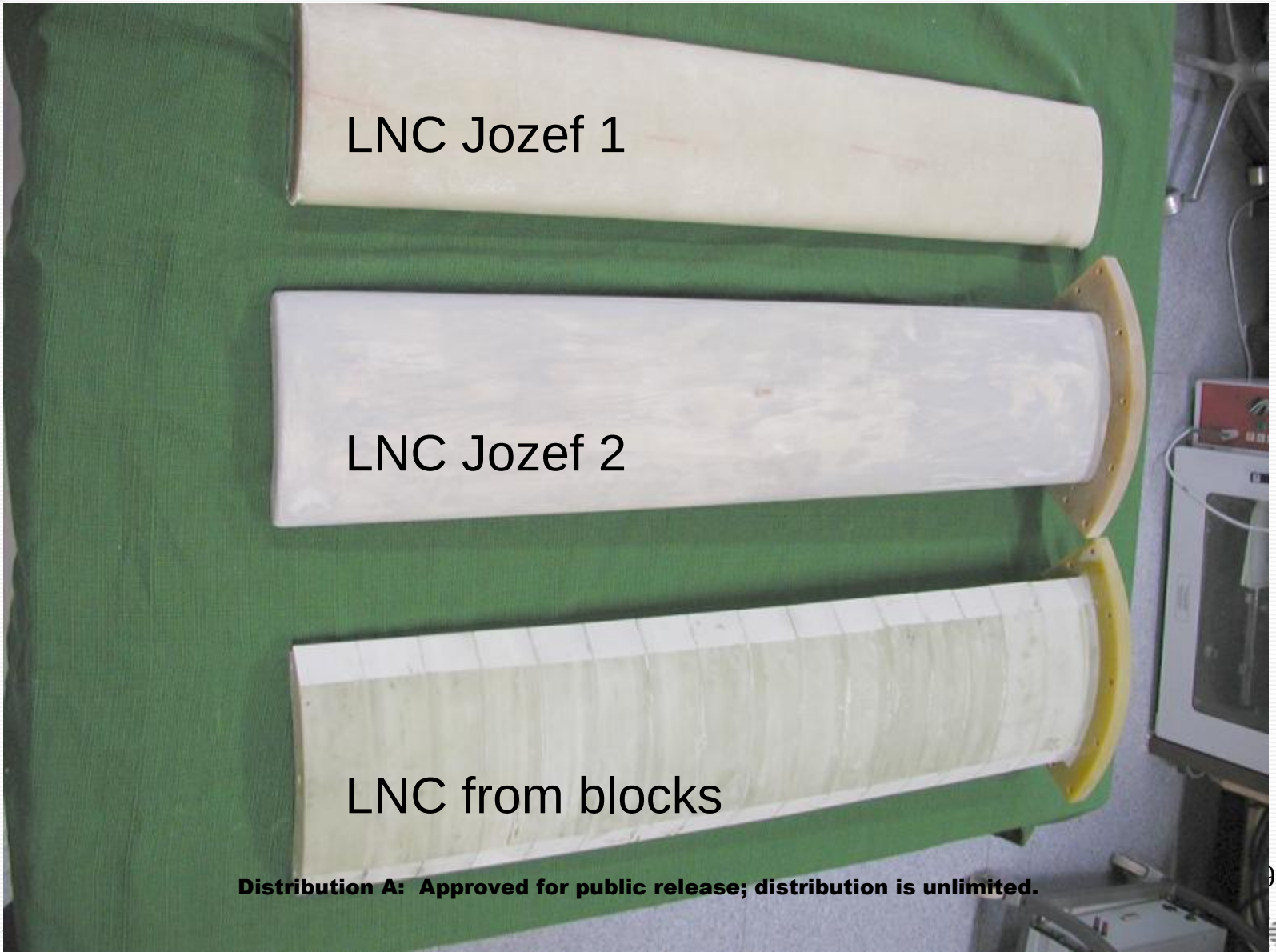

Drawings of the device, photographs

Final version of the LN_2 container

Drawings of the device, photographs

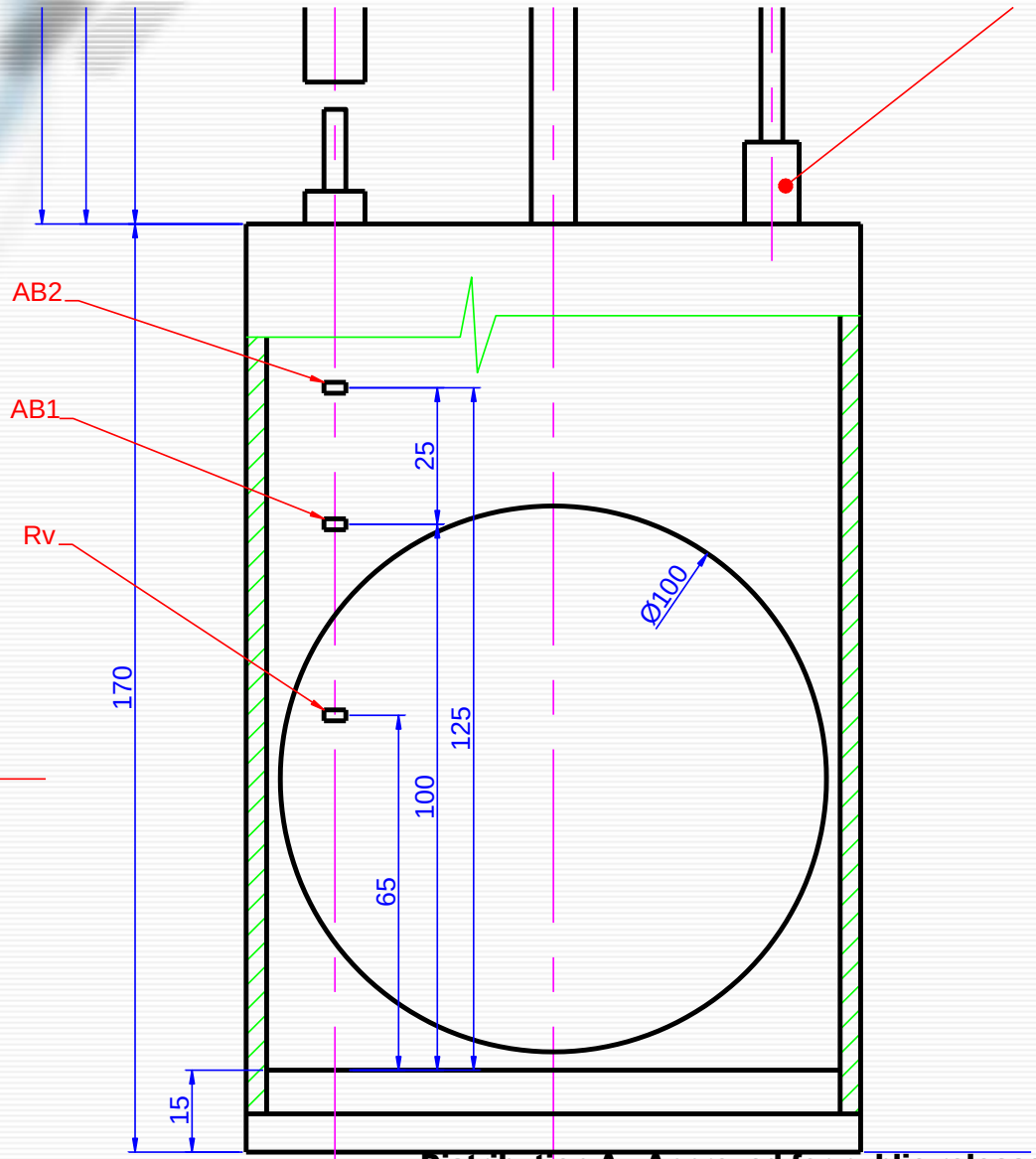

Inside of the calorimeter box

A

Test results

We realized the following tests:

1. Mechanical deformation of the liquid nitrogen container (LNC) at 300 K
2. Vacuum tightness of the LNC
3. Evaporation rate of N_2 for LNC placed in vacuum space
4. Tests of the complete device (LNC + calorimeter box)

Mechanical deformation of the liquid nitrogen container (LNC) at 300 K

3 types of containers were tested:

- blocks glued together
- Laminated, old epoxy
- Laminated, Epoxy CHS 1200

Results: The last version showed deformation smaller than 1.5 mm at 300 K, even smaller deformation is expected at 77 K

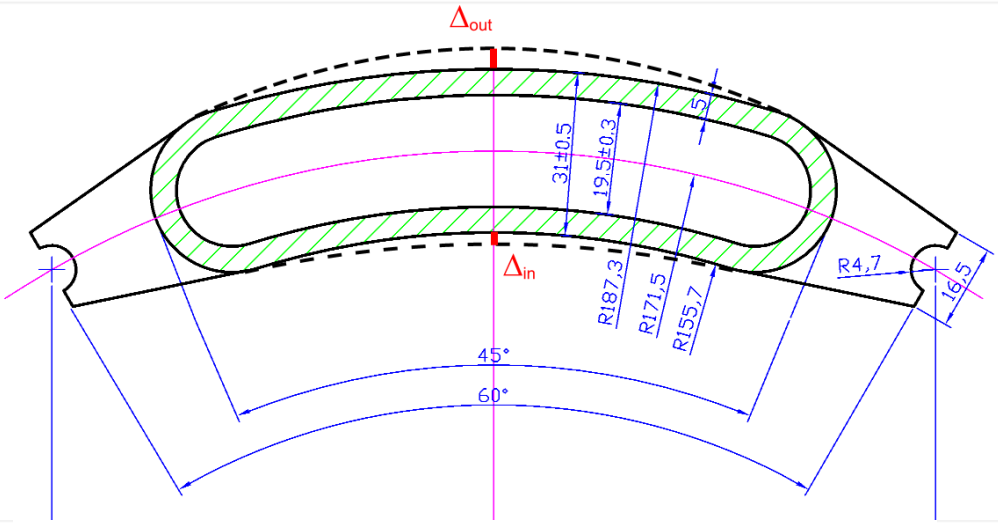

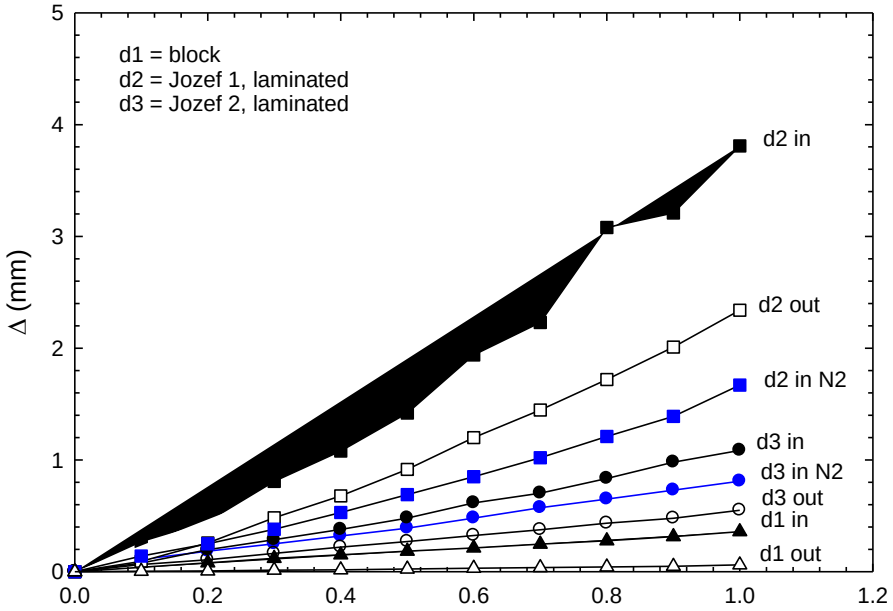

p kp/cm2 vs d3 vnut N2

Vacuum tightness of the system

The container Jozef 2 was placed in a working space of a metallic cryostat with the inner diameter of 200 mm. The space outside the container (the working space of the cryostat) was evacuated using pumping system AV63 (pumping speed of 110 l/sec in the pressure interval 10^{-1} to 10^{-3} Pa).

We note that the pumping system was manufactured in year 1982 and it is not in a very good shape). A vacuum of ~ 20 Pa was achieved 40 minutes after the start of the pumping approximately.

Evaporation rate of N_2 for LNC placed in vacuum space

Vessel Jozef 2,
time decay of the LN2 level
26. february 2010

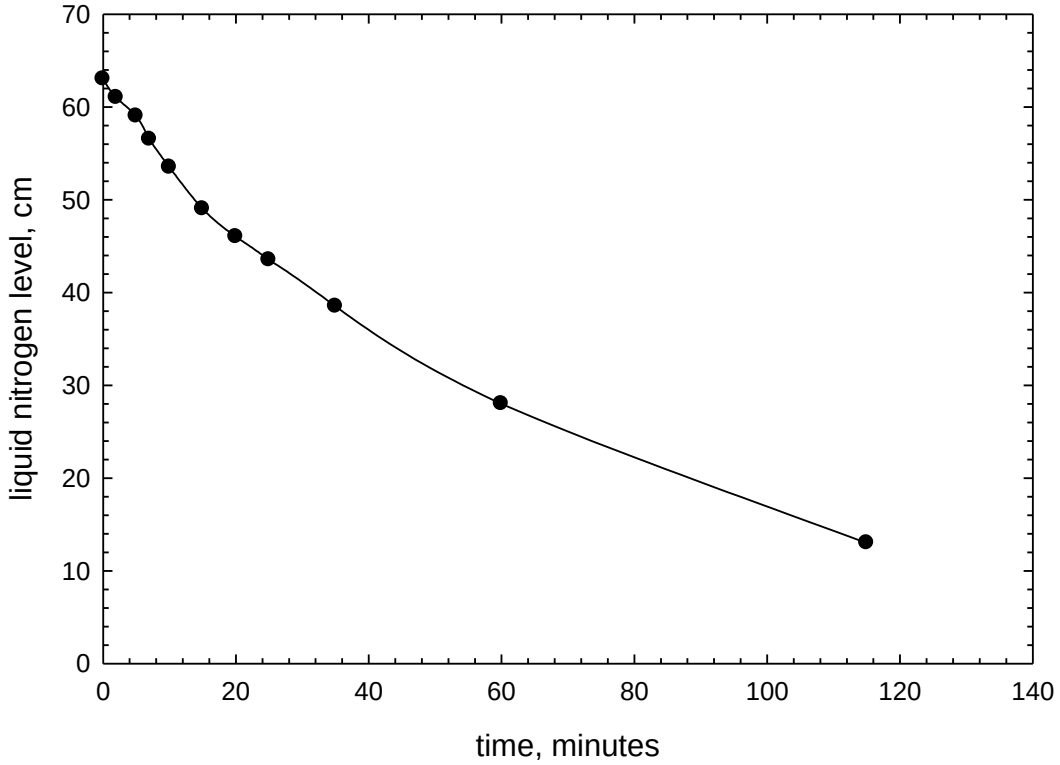

We measured the decay of liquid N_2 level; the starting level was ~ 650 mm (measured from the bottom of LNC)

Still of 350 mm of LN_2 was measured after 40 minutes without refilling of the container

Tests of the complete device (LNC +calorimeter box)

Calorimeter box "2"
Calibration, 21. 6. 2010
R_{heater}=104 Ohm

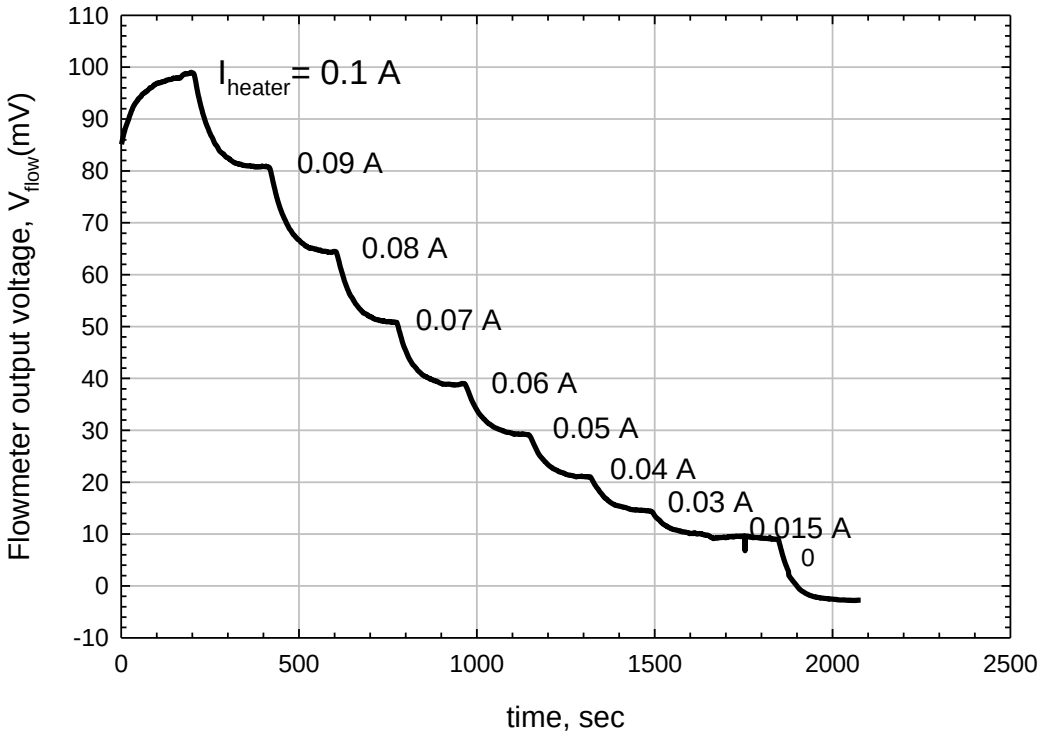

Flowmeter output voltage vs. time for various decreasing heating power
P_h= 104 $(I_{heater})^2$ + 0.1645 W
A constant additional heating of 164.5 mW was used.

We heated the interior of the calorimeter box by additional constant heating power of 164.5 mW

Total heating power

$P_h = 164.5\ mW + R_{heat} x\ I_{heat}^2$

Than, we set down the heating power stepwise (as indicated in the figure)

The time needed to reach the saturated state is about 5 to 7 minutes

Calibration curve with and without additional heating

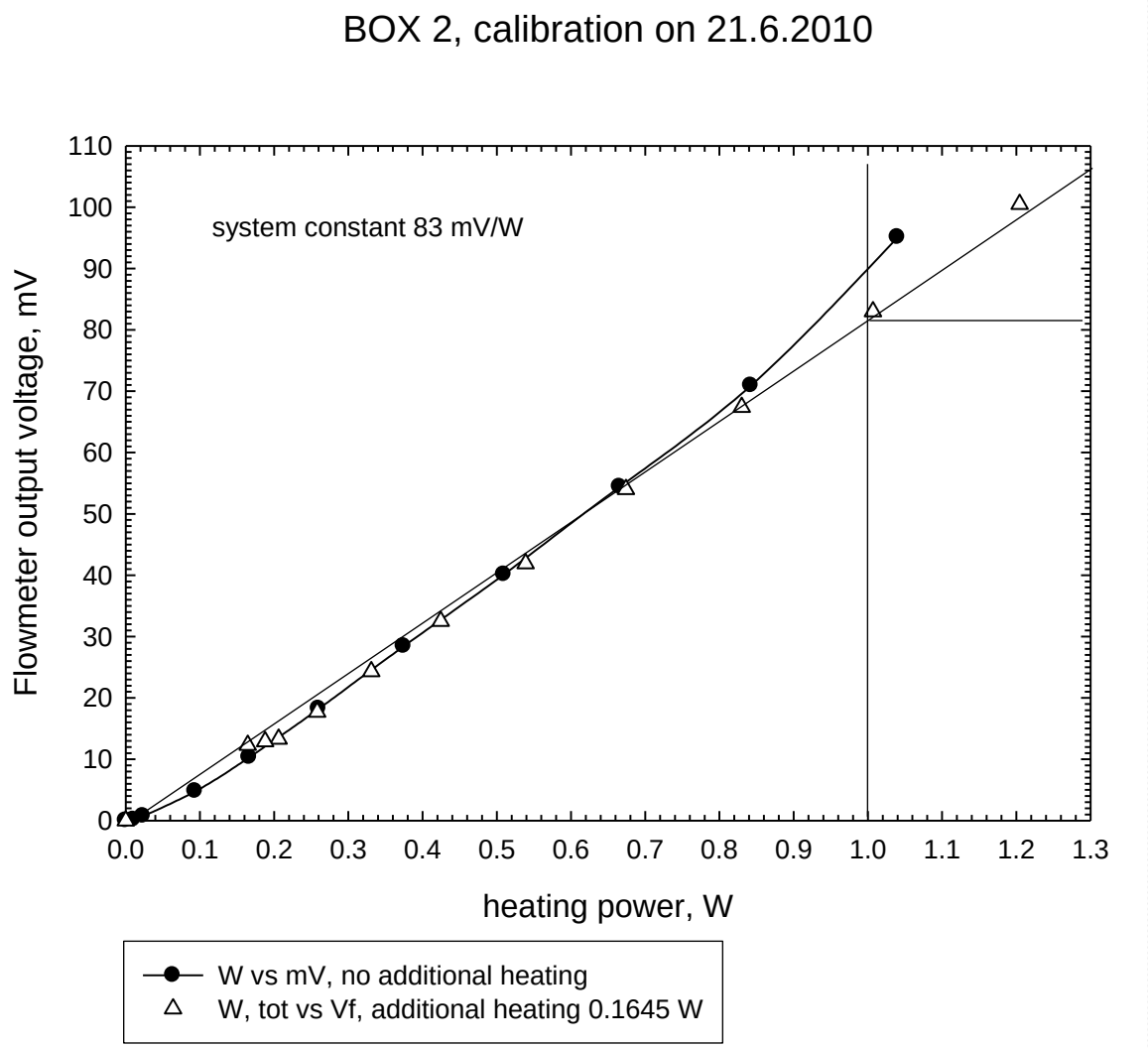

The linearity of the calibration curve: Output voltage of the flowmeter vs. heating is considerably improved using additional heating

Conclusions

The calibration of the calorimeter box showed that the output voltage of a flowmeter (Setaram in our case) is nearly proportional to the heating power. The constant is 83 mV/mW.

Using an additional constant heating of about 150 mW improves the stability of the system thanks to a homogeneous distribution of bubbles inside the box.

In our system the slow decrease of the liquid nitrogen level allowed continuous measurements of losses of about 30 to 40 minutes